Origin, Reactivity, and Bioavailability of Mercury in Wildfire Ash

By: Peijia Ku, Martin Tsz-Ki Tsui, Xiangping Nie, Huan Chen, Tham C. Hoang, Joel D. Blum, Randy A. Dahlgren, and Alex T. Chow

Ku, Peijia; Tsui, Martin Tsz Ki; Nie, Xiangping; Chen, Huan; Hoang, Tham C.; Blum, Joel D.; Dahlgren, Randy A.; Chow, Alex T. Origin, Reactivity, and Bioavailability of Mercury in Wildfire Ash. *Environmental Science and Technology*. v52 n24 (Dec 18, 2018) 14149-14157. https://doi.org/10.1021/acs.est.8b03729

Abstract:

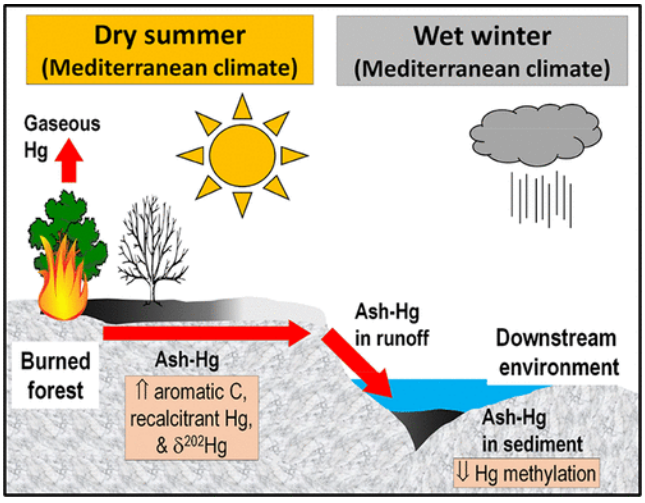

Wildfires are expected to become more frequent and intensive at the global scale due to climate change. Many studies have focused on the loss of mercury (Hg) from burned forests; however, little is known about the origins, concentration, reactivity, and bioavailability of Hg in residual ash materials in postfire landscapes. We examine Hg levels and reactivity in black ash (BA, low burn intensity) and white ash (WA, high burn intensity) generated from two recent northern California wildfires and document that all ash samples contained measurable, but highly variable, Hg levels ranging from 4 to 125 ng/g dry wt. (n = 28). Stable Hg isotopic compositions measured in select ash samples suggest that most Hg in wildfire ash is derived from vegetation. Ash samples had a highly variable fraction of Hg in recalcitrant forms (0–75%), and this recalcitrant Hg pool appears to be associated with the black carbon fraction in ash. Both BA and WA were found to strongly sequester aqueous inorganic Hg but not gaseous elemental Hg under controlled conditions. During anoxic ash incubation with natural surface water, we find that Hg in most ash samples had a minimal release and low methylation potential. Thus, the formation of wildfire ash can sequester Hg into relatively nonbioavailable forms, attenuating the potentially

adverse effects of Hg erosion and transport to aquatic environments along with eroded wildfire ash.

Keywords: wildfire ash | mercury (Hg) | adsorption | bioavailability

Article:

Introduction

Wildfire is an important ecosystem perturbation affecting ∼3% of the global vegetated land surface each year.(1) Because of climate change, wildfire is predicted to be more frequent and intense this century in semiarid regions including California, Australia, and the Mediterranean region of Europe.(2−5) Forest ecosystems not only represent an important sink for atmospheric mercury (Hg), but also are a source of Hg to the environment through biomass burning and runoff.(6) Wildfire can lead to substantial loss of Hg previously sequestered in vegetation, surficial detritus, and topsoil to the atmosphere, predominantly in the form of gaseous elemental Hg(0).(7−9)

Despite the prevalence of studies focusing on Hg loss during wildfires, one aspect of wildfire effects on Hg cycling has received very little attention: the concentrations and reactivity of Hg in burned biomass residues (i.e., wildfire ash). To our knowledge, there are only two prior studies reporting Hg levels in wildfire ash. Engle et al.(10) found that ash had 39.2 ng/g of Hg (on a dry mass basis) compared to 91.4 ng/g in unburned forest litter in western Nevada (USA); however, it should be noted that ash samples were collected almost a year after the wildfire and the results may have been compromised by subsequent rainfall, runoff, and leaching. Campos et al.(11) collected wildfire ash 4 weeks after burning from two sites in Portugal that had different burn intensities and found ash with significantly more Hg in areas of moderate burning (112 ng/g) compared to ash in areas with high intensity burning (64 ng/g). In contrast, studies using controlled biomass burning under oxygenated conditions consistently found ash with very low Hg content, ranging from 0.4 to 11.1 ng/g (on a dry mass basis),(8,12) raising questions regarding the factors controlling the Hg content of wildfire ash.

On the basis of color and percent loss-on-ignition (LOI),(11,13) wildfire ash can be operationally divided into two major classes: black ash (BA; low intensity fire; 200–500 °C) and white ash (WA; high intensity fire; > 500 °C).(13) However, it should be noted that within each class, ash may consist of a mixture of materials with contrasting mineral and organic matter contents. In essence, BA is generated by incomplete combustion of biomass, while WA is produced by more complete combustion.(14) BA is known to contain appreciable amounts of charcoal or black carbon (BC), while WA generally contains high mineral concentrations that can be dominated by $CaCO_3$, CaO, or aluminosilicates.(13,15) As related to Hg cycling, it is essentially unknown how BC in wildfire ash mediates Hg levels, reactivity, and bioavailability. The wildfire ash layer is highly susceptible to runoff-leaching and erosional processes due to the lack of soil cover and the fine powdery nature of the ash materials, thereby resulting in a strong potential for transporting Hg in the wildfire ash to aquatic environments including streams, lakes, and reservoirs.(16,17) In particular, one area of concern is whether Hg in ash is available for microbial methylation when ash is deposited in anoxic zones, which can serve as biogeochemical hotspots of Hg methylation

(e.g., biofilms(18)). Methylmercury (MeHg) can form under anoxic conditions(19) and is highly bioaccumulative, thus elevating MeHg levels in downstream biota.(20)

The overall goal of this study was to provide the first rigorous characterization of Hg in ash by collecting and analyzing ash from two wildfires (Wragg and Rocky Fires) in northern California. Specifically, we examined (i) Hg levels and Hg reactivity using two acid digestion methods as an operationally defined measure of Hg reactivity in ash and compared results with unburned vegetation (i.e., the potential fuel load); (ii) the isotopic composition of Hg in wildfire ash to provide further insights to the origins of Hg in ash; (iii) the capability of wildfire ash to adsorb ambient Hg (both aqueous and gaseous Hg) due to the "higher-than-expected" Hg content in many wildfire ash samples compared to lab-generated ash;(8,12) and (iv) the bioavailability of Hg released from wildfire ash to methylating microbes to determine whether wildfires might stimulate Hg methylation in downstream aquatic environments.

Materials and Methods

Sample Collection

We collected wildfire ash samples 3–5 weeks following two northern California wildfires in the summer of 2015: the Wragg Fire and the Rocky Fire (see site characteristics and specific sampling points in Supporting Information Table S1). No rainfall occurred between the fire and the sampling, and thus, the ash samples were not eroded or leached by rainfall or runoff.(10,13) Paired ash samples [i.e., black ash (BA) and white ash (WA) were visually distinguished in the field](21) were collected at each site (5 pairs for the Wragg Fire, and 9 pairs for the Rocky Fire). Surface ash samples (generally 0–5 cm) were carefully collected to avoid mixing with underlying soil using a stainless-steel hand shovel and were then placed into a clean polyethylene bag. It should be noted that BA and WA characterization represents the dominant materials visually identified in the field, but they should not be considered pure endmembers as there is significant short-range spatial variability in both the horizontal and vertical dimensions of the ash layer.(13) At the landscape scale for both sites, we estimated that ∼90% of the surface contained BA and ∼10% WA, which was a function of local fuel load distribution (e.g., proximity to tree trunks). In general, we expected that the surface materials would be burned at a higher temperature and at more oxygenated conditions than the deeper ash layers leading to inherent variability within the vertical dimension. Unburned vegetation (twigs and branches) and surface litter were collected as a control from the dominant tree species in unburned areas located adjacent to the fire perimeter (see locations in Table S1). We present the data for each individual ash sample since there was a large heterogeneity among samples within each ash category (BA or WA; originally considered as replicates).

Ash Characterization and Analyses

All ash samples were dry at the time of collection and therefore did not require further drying in the laboratory. Ash samples were heterogeneous in size, shape, and color of materials (especially BA; see pictures of presieved and 2 mm sieved ash, Figure S1) and were therefore sieved through a 2 mm acid-cleaned polypropylene mesh and thoroughly homogenized. Unburned litter and dead woody materials were frozen, freeze-dried, and homogenized (<2 mm) using a

stainless-steel grinder. All samples were analyzed for color using a Munsell color chart(22) (except unburned vegetation materials), and ash color was assigned according to Bodí et al.(23) LOI was determined using a muffle furnace and total calcium (Ca) using an ICP-MS. The chemical composition of organic carbon was characterized using pyrolysis-GC/MS to provide semiquantitative (relative) levels of BC(24−26) as defined here by the fraction of aromatic hydrocarbon (ArH).(15) It should be noted that the combustion temperature of LOI was set at 500 °C to prevent the loss of dominant inorganic components such as carbonate (e.g., 600–800 °C),(27) and thus, we regard LOI as a proxy of organic matter content in the samples. Procedural details of these analyses are found in SI Text 1.

We determined total-Hg concentrations using two digestion methods: Method 1 (reported as [$Hg_{method\text{-}1}$]; targeting organic matter-bound-Hg) used trace-metal grade HNO_3 and H_2O_2 (4:1, v:v) in a 80 °C water bath overnight, and Method 2 (reported as [$Hg_{method\text{-}2}$]; targeting all geochemical pools) used aqua regia (freshly mixed trace-metal grade HNO_3 and HCl, 1:3, v:v). See SI Text 2 for detailed Hg analytical methods. On the basis of previous studies on soils and sediments, digestion methods (e.g., hot HNO_3 and H_2O_2) similar to Method 1 would not result in digestion of charcoal or BC from environmental samples;(28,29) thus, it may potentially allow us to distinguish Hg bound to organic matter versus Hg bound to BC in ash samples, while Method 2 (aqua regia) is expected to result in digestion of recalcitrant BC from the samples. On the basis of previous sequential extraction studies on Hg, [$Hg_{method\text{-}1}$] includes Hg from all pools except recalcitrant geochemical pools, which include HgS and HgSe, while [$Hg_{method\text{-}2}$] should also include Hg from recalcitrant geochemical pools,(30,31) but we found no study reporting whether BC-bound Hg belongs to the recalcitrant geochemical pools. On the basis of the above rationale, we operationally defined the "recalcitrant" pool of Hg as

$$\text{Recalcitrant Hg (\%)} = [1 - (Hg_{method-1}/Hg_{method-2})] \times 100$$

We compared [$Hg_{method\text{-}2}$] and Hg reactivity in ash samples to unburned biomass samples (collected postburn). To assess the robustness of our approach for estimating Hg reactivity, we included two standard vegetation reference materials (SRMs) and previously characterized litter samples from three reference forests in northern California Coast Range, northern Michigan, and central New Hampshire (see SI Text 2). We estimated the degree of Hg volatilization from the burned biomass using a mass balance with LOI and Ca content in the ash (see SI Text 3 for details). Further, we processed 10 ash samples from the Wragg Fire (5 BA and 5 WA) along with litter from the reference forests for stable Hg isotopic composition using a thermal combustion procedure to gain further insights regarding the origins and transformations of Hg in ash (see SI Text 4 for details).

To determine if wildfire ash can adsorb ambient Hg, we used wildfire ash samples from the Wragg Fire to determine the Hg sorption potential of gaseous Hg [as elemental Hg(0)] and aqueous Hg [as inorganic Hg(II)] (see SI Text 5 for details). We also used activated carbon as a reference sorbent for comparison to the ash materials.

To determine the release and potential bioavailability of Hg associated with wildfire ash for microbial methylation, we conducted a sealed incubation experiment similar to Tsui et al.(32) by incubating an unburned litter sample from the reference forest in the northern California coast

range and BA and WA from both wildfires in natural streamwater for 4 and 12 weeks (see SI Text 6). At the end of the incubation period, aqueous samples were filtered (using prebaked Whatman GF/B filters; 1.0-μm pore size) and analyzed for various physiochemical parameters including the presence or absence of a sulfidic smell (an indicator of anoxic conditions), pH, dissolved organic carbon (DOC), UV absorbance (to calculate $SUVA_{254}$, a proxy of DOC aromaticity), total dissolved nitrogen (TDN), dissolved Hg, and dissolved MeHg.

Statistical differences ($p < 0.05$) between two groups were evaluated by student's *t* test, and differences between multiple groups were assessed using one-way ANOVA with a posthoc Tukey's Test. Regression analyses were conducted using SigmaPlot 12.5.

Results and Discussion

Chemical Properties and Mercury Content of Ash

We found that the LOI value decreased in the order: unburned litter/woody materials (∼95%) > BA (23–62%) > WA (3–15%) (Figure 1A) ($p < 0.05$), which was consistent with our expectation of decreasing organic matter content with higher burn intensity.(11,13) Consistent with other reports,(15) the Ca content in ash was significantly elevated for BA and WA ($p < 0.05$) compared to unburned samples (Figure 1B) and Ca was significantly higher in WA than BA ($p < 0.05$). Black carbon (BC), defined here as the aromatic hydrocarbon (ArH) fraction, decreased in the order: WA > BA > unburned samples ($p < 0.05$; Figure 1C). In general, ArH was negatively and significantly correlated with LOI among ash samples ($p = 0.0013$; Figure S2). These results suggest that increasing burn intensity resulted in ash with a higher proportion of BC, which is consistent with studies that examined water extracts of ash materials.(33)

We report Hg concentrations of samples digested with aqua regia (i.e., $[Hg_{method\text{-}2}]$), as this digestion method releases the most Hg from different geochemical pools.(30,31,34) Similar to vegetation samples across a large geographic gradient in the United States,(35) we found only a narrow range of $[Hg_{method\text{-}2}]$ for litter (20.3–40.1 ng/g in study sites; 35.0–57.8 ng/g in reference forests) and dead woody materials (14.6–57.0 ng/g in study sites) (Figure 1D). The $[Hg_{method\text{-}2}]$ among all ashes ranged from 3.9 to 124.6 ng/g ($n = 28$) (Figure 1D), with many samples having $[Hg_{method\text{-}2}]$ higher than ash generated in lab studies.(8,12) We detected no significant differences in $[Hg_{method\text{-}2}]$ among unburned samples, BA, and WA ($p > 0.05$) (Figure 1D). We found that the pool of "% recalcitrant Hg" averaged 7.6% among all unburned samples tested (Figure 1E; Table S2). In contrast, BA samples had highly variable, but significantly higher, "% recalcitrant Hg" than both unburned and WA samples ($p < 0.05$), while WA samples (Rocky Fire only) had an intermediate-sized pool of "% recalcitrant Hg" (Figure 1E).

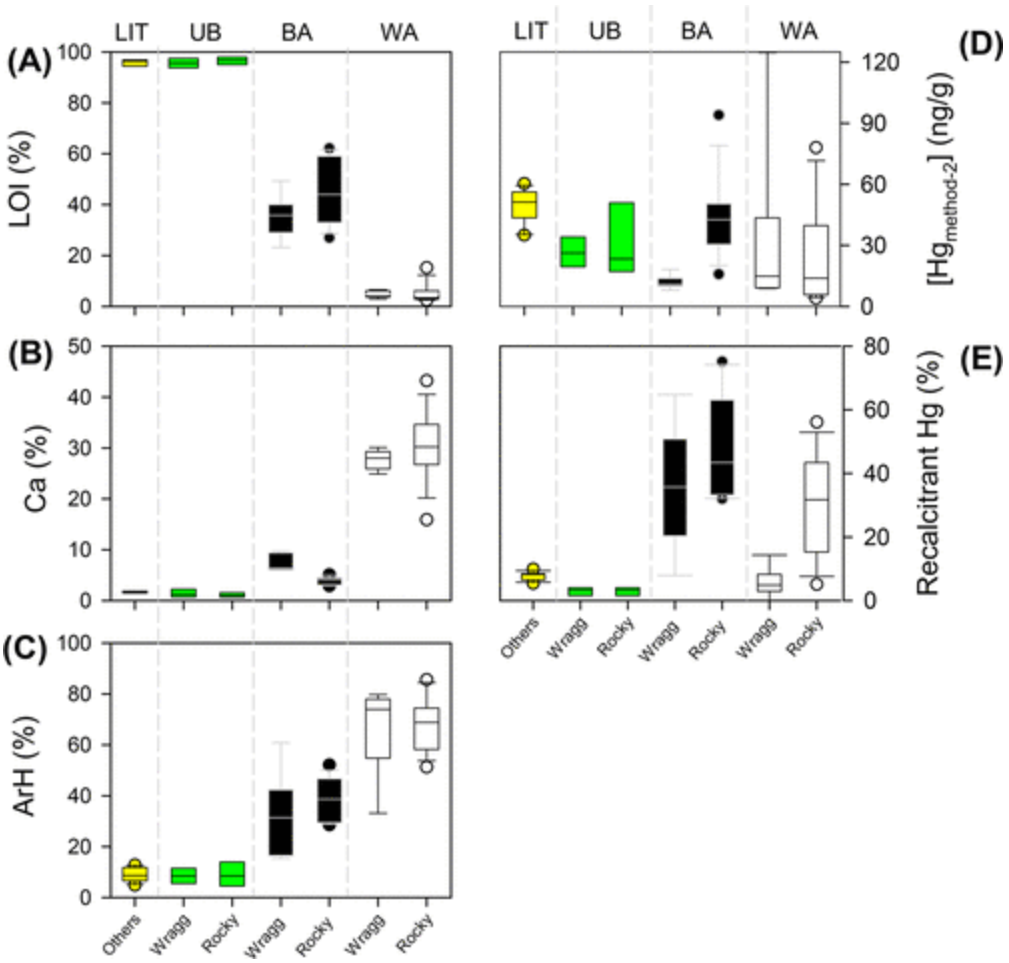

Figure 1. Box plots of (A) loss-on-ignition (LOI), (B) calcium (Ca), (C) pyrolysis products (via Py-GC-MS analysis) as fraction of aromatic hydrocarbon (ArH), (D) Hg concentrations based on digestion method 2, aqua regia ($Hg_{method-2}$), and (E) percent recalcitrant Hg, in unburned litter ("LIT") from the three reference forests ("others") in yellow, litter/wood from the two fire sites ("UB"; in green; $n = 2$ of litter and $n = 2$ of wood per site), black ash ("BA"; in black; $n = 5$ for Wragg, and $n = 9$ for Rocky), and white ash ("WA"; in white; $n = 5$ for Wragg, and $n = 9$ for Rocky).

The negative relationship (significant for Rocky Fire samples only; $p < 0.05$) between LOI and "% recalcitrant Hg" in BA from both the Wragg and Rocky Fires (Figure 2A) may help explain some variations of Hg reactivity in ash samples. Such relationships between LOI and "% recalcitrant Hg" were absent among WA samples (Figure 2B). For BA samples, we posit that increased burn intensity lowered LOI, and thus, potentially more BC was generated due to limited oxygen availability. It is intriguing that we find a positive linear correlation between ArH and "recalcitrant Hg" among all BA and unburned samples (i.e., $r^2 = 0.896$, $p < 0.001$) (Figure 2C). However, we found no such relationship for WA samples ($p > 0.05$) (Figure 2D).

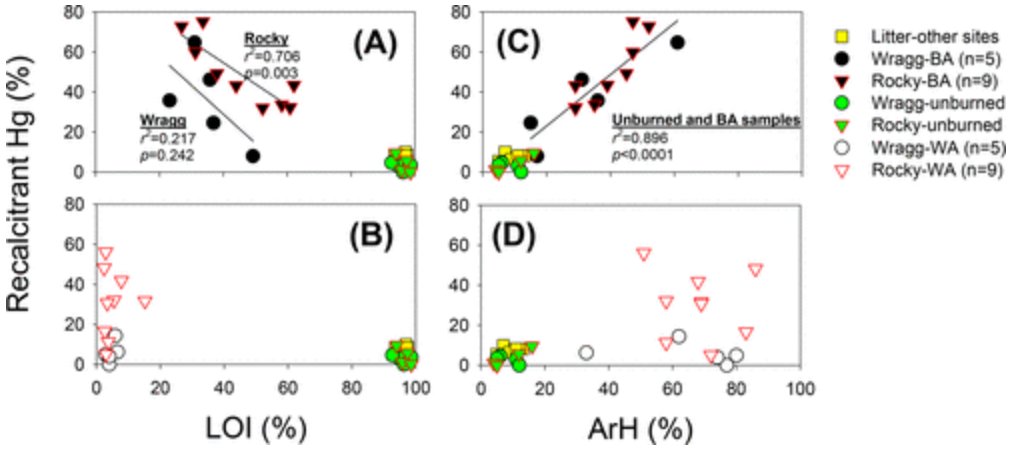

Figure 2. Relationships between loss-on-ignition (LOI) and percent recalcitrant Hg in (A) unburned materials and black ash (BA) and (B) unburned materials and white ash (WA), and relationships between aromatic hydrocarbon (ArH) fraction of pyrolysis products and percent recalcitrant Hg in (C) unburned materials and BA and (D) unburned materials and WA. Unburned samples are litter from three reference forests (as "Others"; in yellow) as well as litter/wood from the two fire sites (in green, different symbols).

Apparently wildfire increased the occurrence of benzene-ring containing organic compounds in burned biomass such as the aromatic hydrocarbon (ArH) fraction determined in this study. Aromatic hydrocarbons are known to have a high affinity for trace metals(36) as a result of stable pi-complexes between aromatic hydrocarbon ligands and metals.(37) Meanwhile, the lack of a relationship between ArH and recalcitrant Hg in WA may be attributed to the fact that the absolute abundance of OC in WA is very low (e.g., assuming half of the LOI is OC). Thus, even WA has a high fraction of ArH (Figure 1C), and the absolute abundance of ArH is still low and has a narrow range of absolute ArH abundance (inferred by small range of LOI) among WA samples, which may weaken the regression relationship between %ArH and "% recalcitrant Hg" (Figure 2D).

Extent of Hg Volatilization upon Burning

Since Ca was significantly elevated ($p < 0.05$) in BA and WA compared to unburned samples from the Wragg and Rocky Fires, we performed a simple mass balance calculation to estimate Hg volatilization losses from the preburn fuel loads based on LOI and Ca in ash as compared to their unburned counterparts. We assumed a constant LOI of ~95% for the unburned fuels (based on our measured values of unburned materials) and that Ca was conserved during wildfires regardless of temperature and oxygen conditions (see equations in SI Text 3). BA and WA samples from the Wragg Fire (Figure 3 and Table S3) indicated ≥80% Hg loss compared to the fuel samples. WA in the Rocky Fire had estimated Hg losses of ≥90%, but interestingly, BA from the Rocky Fire had a wide range of Hg loss estimates from 34 to 83%. As previously noted, BA samples may contain materials originating from a wide range of fire conditions (temperature and oxygen levels) resulting in a mixture of highly contrasting ash materials in the horizontal and vertical dimensions. These results suggest that fire intensity and burning conditions (i.e., temperature, oxygen availability, and duration) are important in determining Hg volatilization. Although we estimated Hg volatilization in individual samples in the present study, it should be

noted that Hg volatilization/emission can be estimated in the field at the landscape level, but this would require the estimation of the total amount of fuel loss.(38)

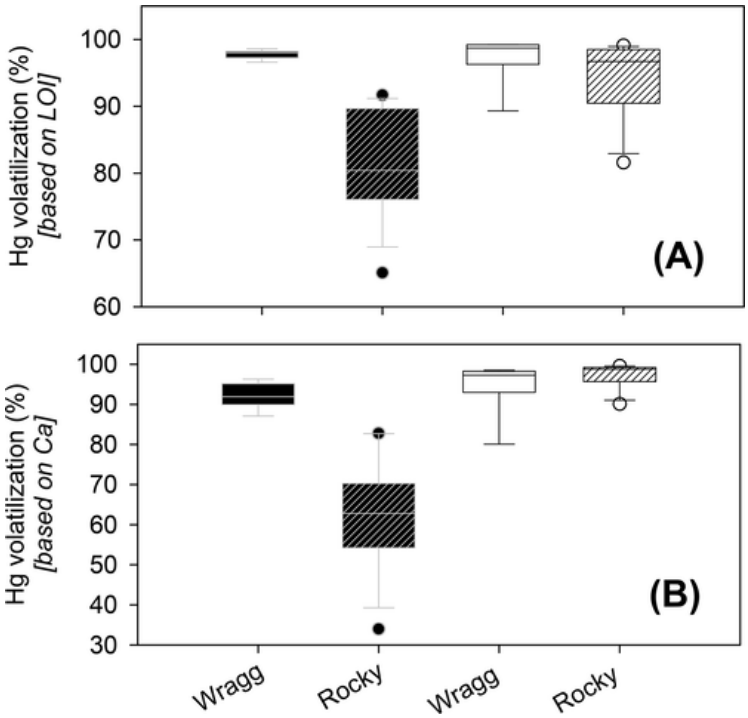

Figure 3. Box plots of estimated mercury (Hg) volatilization from original fuel loads (assumed to be a mixture of litter and dead woody materials) in the Wragg Fire (2015) and the Rocky Fire (2015) based on (A) loss-on-ignition (LOI) and (B) calcium (Ca) content of ash samples. Note: Wragg Fire black ash (in black bars), Wragg Fire white ash (in white bars), Rocky Fire black ash (in hatched black bars), and Rocky Fire white ash (in hatched white bars). See Table S3 for the individual ash data.

Isotopic Composition and Source Analysis of Hg in Ash

Forest litter in the unburned reference forests for this study and foliage from another study(39) along a large geographic gradient in North America all show a relatively narrow range of δ^{202}Hg (MDF; mass-dependent fractionation) and Δ^{199}Hg (MIF; mass-independent fractionation) (Figure 4; Table S4). Since forests receive Hg predominantly from atmospheric deposition, we expect Hg isotopic compositions in the unburned vegetation materials (foliage, litter, and dead wood) to be similar to the MDF and MIF values of our reference sites. Both BA and WA from the Wragg Fire had very different Hg isotopic compositions compared to litter and foliage samples as well as gaseous Hg samples from other studies (Figure 4). Mean δ^{202}Hg values (MDF) followed the order: unburned (-2.25 ± 0.22 ‰, $n = 16$) < BA (-1.74 ± 0.27 ‰, $n = 5$) ≈ WA (-1.30 ± 0.47 ‰, $n = 5$) (Figure 4). The higher δ^{202}Hg values in ash samples are consistent with our expectation that lighter Hg isotopes are preferentially volatilized by fire while the heavier isotopes are concentrated in the residual ash, slightly more so for WA than BA (by an average of 0.44 ‰, Figure 4). However, it should be noted that there were large variations in δ^{202}Hg, even within each ash sample type (WA vs BA), suggesting mixing of partially burned and unburned materials in BA. Importantly, δ^{202}Hg was significantly correlated with LOI and

ArH content of individual BA and WA samples (Figure S3). Thus, it appears that higher burning intensity leads to higher δ^{202}Hg in the residual ash.

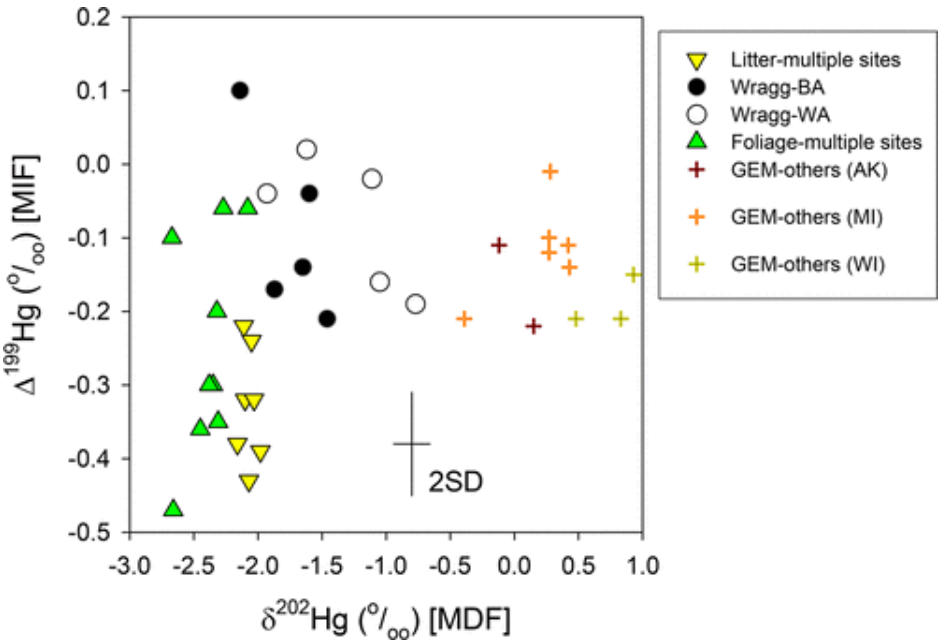

Figure 4. Isotopic composition of mercury (Hg) in unburned forest litter from three reference forests in this study and foliage from Zheng et al.,(39) and black ash (BA) and white ash (WA) collected from the Wragg Fire. Data on gaseous elemental mercury (GEM) were obtained from Gratz et al.(47) for Michigan (MI), Sherman et al.(48) for Alaska (AK), and Demers et al.(49) for Wisconsin (WI). Error bars represent the maximum analytical error associated with sample analysis (2SD).

There was a narrow range of Δ^{199}Hg (MIF) values among litter and foliage samples (−0.47 to −0.06 ‰; Figure 4) and the majority of the ash samples had slightly elevated Δ^{199}Hg values relative to litter and foliage, with one BA sample even having a slightly positive Δ^{199}Hg value (+0.10 ‰). MIF is not expected to occur as a result of combustion (at least in the dark), and is mainly caused by photochemical reactions.(40) Given the very small magnitude of differences among ash and the unburned materials, there is no compelling evidence for significant MIF during burning of biomass in wildfires. However, we cannot fully exclude the possibility that a small amount of MIF may have occurred during the postburn period prior to sampling (3–5 weeks) when a surface layer of ash material was exposed to sunlight in the field. We also cannot rule out a small amount of dark microbial reduction in the soils leading to a very small magnitude of MIF through the nuclear volume mechanism.(41)

Experimental Investigation of Hg Sorption by Wildfire Ash

To assess if the ash, once released into the environment, may interact with ambient forms of Hg, we conducted a controlled experiment to examine how wildfire ash may adsorb “ambient” Hg. We found that activated carbon (n = 1) essentially removed all of the Hg(0) (15 ng per 1.22 g of dry material), consistent with its application to remove Hg(0) from flue gas.(42,43) In contrast, BA (n = 4) and WA (n = 2) removed little Hg(0), averaging 2.0 ± 0.65% and 2.9 ± 3.6% of

Hg(0), respectively (Figure 5 and Table S5). In contrast to the "weak" sorption of gaseous Hg(0) by ash, very strong sorption of aqueous Hg(II) (at 70.3 ng/L in 100 mL solution, per 1 g of materials) was measured using both BA (final Hg(II): 5.3 ± 3.1 ng/L; removal: 92.5 ± 4.4%; n = 4) and WA (final Hg(II): 5.2 ± 4.9 ng/L; 92.7 ± 7.0%; n = 4) (Figure 5), compared to the nearly 100% sorption of Hg(II) by activated carbon (0.01 ng/L; removal: ∼100%), which is similar to previous results.(44)

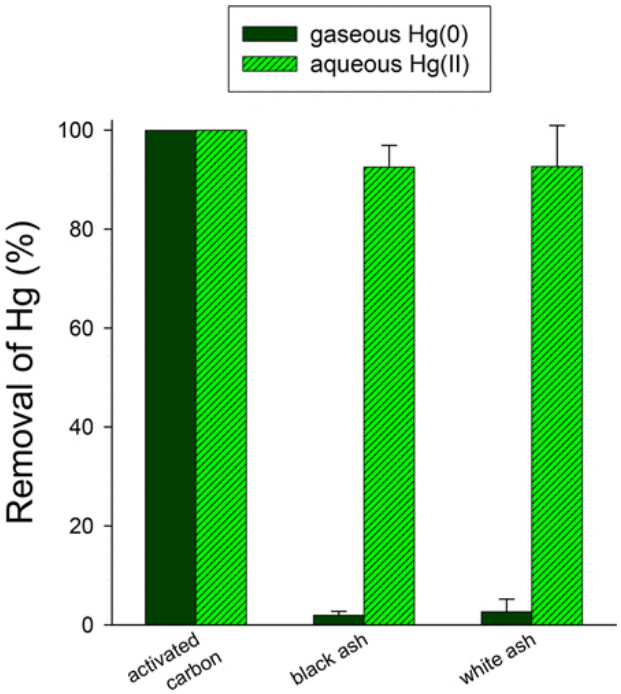

Figure 5. Removal of gaseous Hg(0) (at 15 ng per test, passing through an average of 1.22 g of sorbent) and aqueous Hg(II) (at ∼7–7.5 ng per test with 1.0 g of sorbent) by activated carbon (n = 1 for both tests), black ash from the Wragg Fire (n = 4 for both tests), and white ash from the Wragg Fire (n = 2 for gaseous Hg(0) test and n = 4 for aqueous Hg(II) test). Error bars represent standard deviation.

These results suggest that wildfire ash would not be expected to accumulate Hg(0) in the field (e.g., Hg evasion from underlying soil) and this corroborates the isotopic results given above that indicate Hg in ash is mainly derived from the original vegetation materials. Further, once deposited in aquatic environments, our sorption data suggest that ash can extensively interact with ambient Hg(II) in the water, potentially sequestering ambient Hg(II) into less reactive forms associated with components such as BC. Thus, a higher frequency of wildfire induced by climate change might potentially alter the environmental fate of Hg by producing ash (especially BC) that can sequester Hg(II) in the environment.

Bioavailability of Ash-Associated Hg under Sealed Incubation

We assessed the release and bioavailability of ash-associated Hg for methylation during sealed incubations with freshly collected surface water. This approach of prolonged incubation provides useful information but has some limitations as the resultant water chemistry can change considerably during the course of incubation. For example, the pH of water (beginning pH was

8.0) at the end of the incubations was as follows: litter (5.9 ± 0.64; n = 2) < BA (7.7 ± 0.36; n = 28) < WA (10.0 ± 0.91; n = 28) (Figure S4; Tables S6 and S7). We found that almost all BA or WA samples generated an obvious sulfidic smell, indicating the existence of anaerobic sulfate-reduction across all treatments in addition to the litter-incubated treatment (Tables S6 and S7), which are similar to previous studies.(32,45)

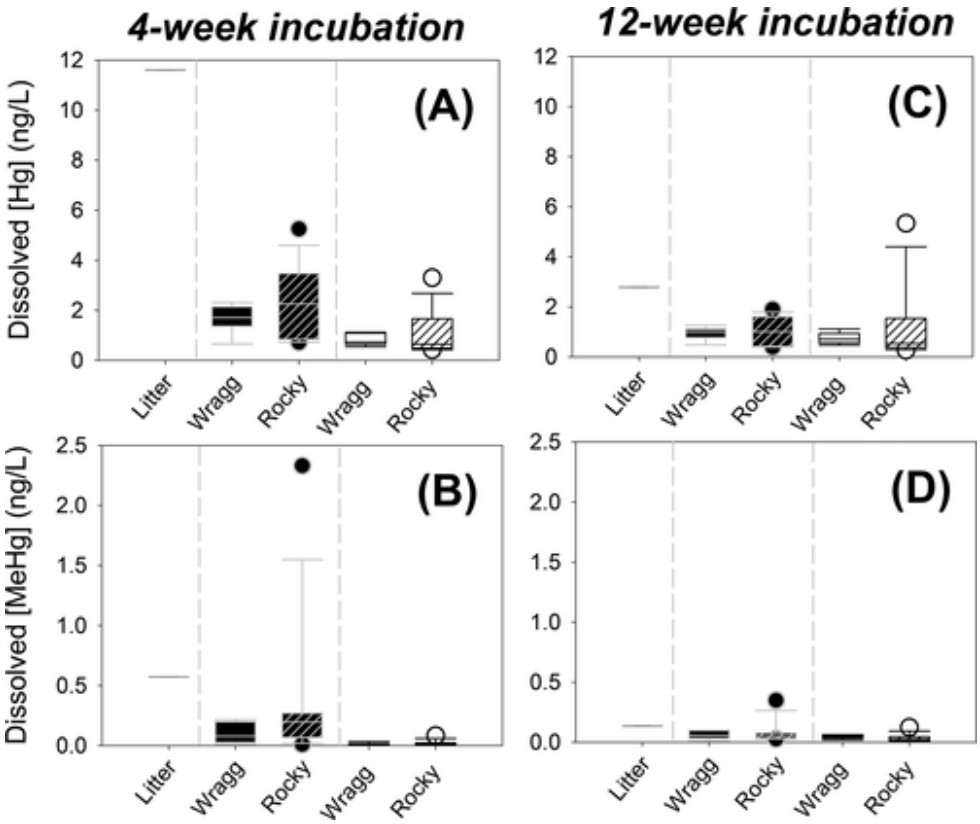

Figure 6. Box plots of (A) dissolved mercury concentrations ([Hg]) after 4 weeks of incubation, (B) dissolved methylmercury concentrations ([MeHg]) after 4 weeks of incubation, (C) dissolved [Hg] after 12 weeks of incubation, and (D) dissolved [MeHg] after 12 weeks of incubation, from an unburned northern California coast range forest litter, Wragg Fire black ash (in black bars), Wragg Fire white ash (in white bars), Rocky Fire black ash (in hatched black bars), and Rocky Fire white ash (in hatched white bars). Individual data points represent triplicate of incubation. See Figure S5 and Tables S6 and S7 for the original data.

Compared to litter incubation (n = 1 with triplicate incubation), we found much lower dissolved (total-) Hg and MeHg in the majority of BA or WA incubation samples after 4- and 12-weeks of incubation (Figure 6 and Figure S5). After 4 weeks of incubation, the percentage of Hg released from the solid materials (after accounting for all Hg pools from water and solid materials) followed the decreasing order: litter (3.3%; n = 1) > BA (0.83 ± 0.50%; n = 14) ≈ WA (0.70 ± 0.57%; n = 14). Importantly, Hg release appeared to be negatively and significantly correlated with the ArH content of the materials (p = 0.002) (Figure S6), implying that "recalcitrant" Hg potentially associated with BC (especially in BA) may limit Hg release into the aqueous phase. However, our interpretation may be confounded by contrasting water quality properties across treatments, such as pH and dissolved organic carbon (DOC) levels (highest in unburned

materials, followed by BA, and then WA-incubations; Figure S4), as these parameters may have an influence on Hg release from these solid materials.

After Hg is leached from the solid-phase, microbial MeHg production may take place in the aqueous phase during incubation under anoxic conditions.(32) In this study, we found that [MeHg] in filtered leachates was consistently low and close to our analytical detection limit of MeHg (0.02 ng/L) for the majority of BA and WA incubations.

However, the dissolved MeHg concentrations for the WA-incubations (and some BA-incubations) appeared to increase with prolonged incubation from 4- to 12-weeks, and these temporal increases were negatively related to the LOI (Figure S7). These results suggest that Hg associated with ligands in WA results in somewhat higher release of Hg from the solid-phase as compared to Hg released from BA during longer incubations. For most BA samples, dissolved Hg, and to a lesser extent MeHg, decreased from 4 to 12 weeks implying that during prolonged exposure aqueous Hg may be "re-adsorbed" onto the ArH pools in BA, or simply accumulate as a solid-phase Hg-sulfide, which has been shown to extensively bind dissolved Hg.(19) We observed similar patterns for litter-incubated treatments ("Litter") with temporal decreases in both dissolved Hg and MeHg (Figure S7), which supports the possibility of sulfidic resorption of Hg.

As demonstrated in our aqueous Hg(II) sorption experiment, both BA and WA had the capability to extensively bind Hg(II) (Figure 5), and this may explain the low release of Hg from BA and WA in the 4-week treatment. In contrast, the 12-week incubation data suggest that sorption from the aqueous phase may be "reversed" such that some of the ash-associated Hg was eventually released back to the ambient water.

Implications for Hg Biogeochemical Cycles

This study demonstrates that the Hg content in wildfire ash is different from ash generated from laboratory-controlled burning investigations.(8,12) We found that the majority of Hg in wildfire ash was derived from Hg that originally resided in vegetation materials (e.g., foliage and litter) based on their Hg isotopic compositions. While the majority (>80%) of the Hg in the litter was volatilized by the fire, considerable concentrations of Hg still existed in the resulting ash. Importantly, pyrolysis appears to generate BC and other constituents that may retain Hg within the residual materials, largely in recalcitrant forms. The recalcitrant forms of Hg in ash appear to sequester additional ambient Hg but inhibit subsequent biogeochemical transformations such as Hg release into solution. Upon deposition into aquatic environments, a small portion of the ash-laden Hg (<1%) is expected to be released based on our incubation data. The extent of Hg release and methylation generally decreased with increasing ArH content, suggesting a possible role of Hg sorption to BC in regulating solubility and bioavailability in the field.

Prolonged exposure to water (especially under reducing conditions) resulted in enhanced Hg release from WA, but a decreased release from BA, highlighting contrasting interactions among ash types generated under different burning conditions on the landscape. Thus, we find that multiple factors (wildfire severity, BC/ArH, length of exposure to water, presence or absence of oxygen, etc.) interact to affect the fate of Hg and determine whether ash serves as a sink or

source of Hg for downstream aquatic environments. Our current findings suggest that wildfire ash could play an important role in global Hg cycling and the Hg biogeochemistry of terrestrial and aquatic ecosystems. For example, wildfire ash itself may decrease or have little effect on Hg contamination in downstream ecosystems (e.g., fish Hg accumulation)(46) due to the less reactive nature of Hg within ash. It should also be recognized that in the burned watersheds other factors such as postburn alteration of food web structures in aquatic ecosystems may lead to subsequent changes in MeHg accumulation in fish.(17) These effects are expected to be more pronounced in the future as climate change results in more frequent and intensive wildfires leading to increasing production of wildfire ash at the global scale.

Acknowledgments

This study was partially supported by a National Science Foundation award to M.T.-K.T. and J.D.B. (DEB-1354811 and DEB-1353850), a National Science Foundation RAPID award to A.T.C. and R.A.D. (CBET-1361678), a National Institute of Food and Agriculture award (2018-67019-27795) to A.T.C. and M.T.-K.T., and a UNC-Greensboro award to P.K. and M.T.-K.T. We thank M. Johnson (University of Michigan) for the expert assistance in stable mercury isotope analysis.

The authors declare no competing financial interest.

References

1. Giglio, L.; Randerson, J. T.; Van der Werf, G. R.; Kasibhatla, P. S.; Collatz, G. J.; Morton, D. C.; DeFries, R. S. Assessing variability and long-term trends in burned area by merging multiple satellite fire products. *Biogeosciences* **2010**, *7*, 1171– 1186, DOI: 10.5194/bg-7-1171-2010 Google Scholar
2. Williams, A. A. J.; Karoly, D.; Tapper, N. The sensitivity of Australian fire danger to climate change. *Clim. Change* **2001**, *49*, 171– 191, DOI: 10.1023/A:1010706116176 Google Scholar
3. Scholze, M.; Knorr, W.; Arnell, N. W.; Prentice, I. C. A climate-change risk analysis for world ecosystems. *Proc. Natl. Acad. Sci. U. S. A.* **2006**, *103*, 13116– 13120, DOI: 10.1073/pnas.0601816103 Google Scholar
4. Westerling, A. L.; Hidalgo, H. G.; Cayan, D. R.; Swetnam, T. W. Warming and earlier spring increase western US forest wildfire activity. *Science* **2006**, *313*, 940– 943, DOI: 10.1126/science.1128834 Google Scholar
5. Marlon, J. R.and many othersWildfire responses to abrupt climate change in North America. *Proc. Natl. Acad. Sci. U. S. A.* **2009**, *106*, 2519– 2524, DOI: 10.1073/pnas.0808212106 Google Scholar
6. Mason, R. P.; Sheu, G. R. Role of the ocean in the global mercury cycle. *Global Biogeochem. Cycles* **2002**, *16*, 1093, DOI: 10.1029/2001GB001440 Google Scholar
7. Friedli, H. R.; Radke, L. F.; Lu, J. Y. Mercury in smoke from biomass fires. *Geophys. Res. Lett.* **2001**, *28*, 3223– 3226, DOI: 10.1029/2000GL012704 Google Scholar

8. Friedli, H. R.; Radke, L. F.; Lu, J. Y.; Banic, C. M.; Leaitch, W. R.; MacPherson, J. I. Mercury emissions from burning of biomass from temperate North American forests: Laboratory and airborne measurements. *Atmos. Environ.* **2003**, *37*, 253– 267, DOI: 10.1016/S1352-2310(02)00819-1 Google Scholar

9. Biswas, A.; Blum, J. D.; Klaue, B.; Keeler, G. J. Release of mercury from Rocky Mountain forest fires. *Glob. Biogeochem. Cycles* **2007**, *21*, GB1002, DOI: 10.1029/2006GB002696 Google Scholar

10. Engle, M. A.; Gustin, M. S.; Johnson, D. W.; Murphy, J. F.; Miller, W. W.; Walker, R. F.; Wright, J.; Markee, M. Mercury distribution in two Sierran forest and one desert sagebrush steppe ecosystems and the effects of fire. *Sci. Total Environ.* **2006**, *367*, 222– 233, DOI: 10.1016/j.scitotenv.2005.11.025 Google Scholar

11. Campos, I.; Vale, C.; Abrantes, N.; Keizer, J. J.; Pereira, P. Effects of wildfire on mercury mobilisation in eucalypt and pine forests. *Catena* **2015**, *131*, 149– 159, DOI: 10.1016/j.catena.2015.02.024 Google Scholar

12. Mailman, M.; Bodaly, R. A. Total mercury, methyl mercury, and carbon in fresh and burned plants and soil in Northwestern Ontario. *Environ. Pollut.* **2005**, *138*, 161– 166, DOI: 10.1016/j.envpol.2005.02.005 Google Scholar

13. Bodí, M. B.; Martin, D. A.; Balfour, V. N.; Santín, C.; Doerr, S. H.; Pereira, P.; Cerdà, A.; Mataix-Solera, J. Wildland fire ash: production, composition and eco-hydro-geomorphic effects. *Earth-Sci. Rev.* **2014**, *130*, 103– 127, DOI: 10.1016/j.earscirev.2013.12.007 Google Scholar

14. DeBano, L. F.; Neary, D. G.; Ffolliott, P. F. *Fire Effects on Ecosystems*; Wiley: New York, 1998. Google Scholar

15. Pereira, P.; Úbeda, X.; Martin, D. A. Fire severity effects on ash chemical composition and water-extractable elements. *Geoderma* **2012**, *191*, 105– 114, DOI: 10.1016/j.geoderma.2012.02.005 Google Scholar

16. Caldwell, C. A.; Canavan, C. M.; Bloom, N. S. Potential effects of forest fire and storm flow on total mercury and methylmercury in sediments of an arid-lands reservoir. *Sci. Total Environ.* **2000**, *260*, 125– 133, DOI: 10.1016/S0048-9697(00)00554-4 Google Scholar

17. Kelly, E. N.; Schindler, D. W.; St. Louis, V. L.; Donald, D. B.; Vladicka, K. E. (2006) Forest fire increases mercury accumulation by fishes via food web restructuring and increased mercury inputs. *Proc. Natl. Acad. Sci. U. S. A.* **2006**, *103*, 19380– 19385, DOI: 10.1073/pnas.0609798104 Google Scholar

18. Battin, T. J.; Besemer, K.; Bengtsson, M. M.; Romani, A. M.; Packmann, A. I. The ecology and biogeochemistry of stream biofilms. *Nat. Rev. Microbiol.* **2016**, *14*, 251– 263, DOI: 10.1038/nrmicro.2016.15 Google Scholar

19. Benoit, J. M.; Gilmour, C. C.; Heyes, A.; Mason, R. P.; Miller, C. L. Geochemical and biological controls over methylmercury production and degradation in aquatic systems. In *Biogeochemistry of Environmentally Important Trace Metals, ACS Symposium Series*

835; Cai, Y., Braids, O. C., Eds.; American Chemical Society: Washington, DC, 2003; pp 262– 297. Google Scholar

20. Tsui, M. T. K.; Finlay, J. C.; Nater, E. A. Mercury bioaccumulation in a stream network. *Environ. Sci. Technol.* **2009**, *43*, 7016– 7022, DOI: 10.1021/es901525w Google Scholar
21. Roy, D. P.; Boschetti, L.; Maier, S. W.; Smith, A. M. S. Field estimate of ash and char colour-lightness using a standard grey scale. *Int. J. Wildland Fire* **2010**, *19*, 698– 704, DOI: 10.1071/WF09133 Google Scholar
22. Munsell Color Company. *Munsell Soil Color Charts*; Macbeth Division of Kollmorgen Corporation: Baltimore, MD, 1998. Google Scholar
23. Bodí, M. B.; Mataix-Solera, J.; Doerr, S. H.; Cerdà, A. The wettability of ash from burned vegetation and its relationship to Mediterranean plant species type, burn severity and total organic carbon content. *Geoderma* **2011**, *160*, 599– 607, DOI: 10.1016/j.geoderma.2010.11.009 Google Scholar
24. De la Rosa, J. M.; Knicker, H.; López-Capel, E.; Manning, D. A.; González-Pérez, J. A.; González-Vila, F. J. Direct detection of black carbon in soils by Py-GC/MS, carbon-13 NMR spectroscopy and thermogravimetric techniques. *Soil Sci. Soc. Am. J.* **2008**, *72*, 258– 267, DOI: 10.2136/sssaj2007.0031 Google Scholar
25. Song, J.; Peng, P. A. Characterisation of black carbon materials by pyrolysis–gas chromatography–mass spectrometry. *J. Anal. Appl. Pyrolysis* **2010**, *87*, 129– 137, DOI: 10.1016/j.jaap.2009.11.003 Google Scholar
26. Chen, H.; Blosser, G. D.; Majidzadeh, H.; Liu, X.; Conner, W. H.; Chow, A. T. Integration of an automated identification-quantification pipeline and statistical techniques for pyrolysis GC/MS tracking of the molecular fingerprints of natural organic matter. *J. Anal. Appl. Pyrolysis* **2018**, *134*, 371– 380, DOI: 10.1016/j.jaap.2018.07.002 Google Scholar
27. Dlapa, P.; Bodí, M. B.; Mataix-Solera, J.; Cerdà, A.; Doerr, S. H. Organic matter and wettability characteristics of wildfire ash from Mediterranean conifer forests. *Catena* **2015**, *135*, 369– 376, DOI: 10.1016/j.catena.2014.06.018 Google Scholar
28. Middelburg, J. J.; Nieuwenhuize, J.; van Breugel, P. Black carbon in marine sediments. *Mar. Chem.* **1999**, *65*, 245– 252, DOI: 10.1016/S0304-4203(99)00005-5 Google Scholar
29. MacKenzie, M. D.; McIntire, E. J. B.; Quideau, S. A.; Graham, R. C. Charcoal distribution affects carbon and nitrogen contents in forest soils of California. *Soil Sci. Soc. Am. J.* **2008**, *72*, 1774– 1785, DOI: 10.2136/sssaj2007.0363 Google Scholar
30. Biester, H.; Scholz, C. Determination of mercury binding forms in contaminated soils: mercury pyrolysis versus sequential extractions. *Environ. Sci. Technol.* **1997**, *31*, 233– 239, DOI: 10.1021/es960369h Google Scholar
31. Bloom, N. S.; Preus, E.; Katon, J.; Hiltner, M. Selective extractions to assess the biogeochemically relevant fractionation of inorganic mercury in sediments and soils. *Anal. Chim. Acta* **2003**, *479*, 233– 248, DOI: 10.1016/S0003-2670(02)01550-7 Google Scholar

32. Tsui, M. T. K.; Finlay, J. C.; Nater, E. A. Effects of stream water chemistry and tree species on release and methylation of mercury during litter decomposition. *Environ. Sci. Technol.* **2008**, *42*, 8692– 8697, DOI: 10.1021/es800956q Google Scholar

33. Wang, J. J.; Dahlgren, R. A.; Ersan, M. S.; Karanfil, T.; Chow, A. T. Wildfire altering terrestrial precursors of disinfection byproducts in forest detritus. *Environ. Sci. Technol.* **2015**, *49*, 5921– 5929, DOI: 10.1021/es505836m Google Scholar

34. Olund, S. D.; DeWild, J. F.; Olson, M. L.; Tate, M. T. Methods for the Preparation and Analysis of Solids and Suspended Solids for Total Mercury. *Techniques and Methods 5 A–8*; U.S. Geological Survey: Reston, VA, 2004. Google Scholar

35. Obrist, D.; Johnson, D. W.; Lindberg, S. E.; Luo, Y.; Hararuk, O.; Bracho, R.; Battles, J. J.; Dail, D. B.; Edmonds, R. L.; Monson, R. K.; Ollinger, S. V.; Pallardy, S. G.; Pregitzer, K. S.; Todd, D. E. Mercury distribution across 14 US forests. Part I: Spatial patterns of concentrations in biomass, litter, and soils. *Environ. Sci. Technol.* **2011**, *45*, 3974– 3981, DOI: 10.1021/es104384m Google Scholar

36. Harrison, R. M.; Tilling, R.; Romero, M. S. C.; Harrad, S.; Jarvis, K. A study of trace metals and polycyclic aromatic hydrocarbons in the roadside environment. *Atmos. Environ.* **2003**, *37*, 2391– 2402, DOI: 10.1016/S1352-2310(03)00122-5 Google Scholar

37. Howell, J. O.; Goncalves, J. M.; Amatore, C.; Klasinc, L.; Wightman, R. M.; Kochi, J. K. Electron transfer from aromatic hydrocarbons and their pi-complexes with metals. Comparison of the standard oxidation potentials and vertical ionization potentials. *J. Am. Chem. Soc.* **1984**, *106*, 3968– 3976, DOI: 10.1021/ja00326a014 Google Scholar

38. Homann, P. S.; Darbyshire, R. L.; Bormann, B. T.; Morrissette, B. A. Forest structure affects soil mercury losses in the presence and absence of wildfire. *Environ. Sci. Technol.* **2015**, *49*, 12714– 12722, DOI: 10.1021/acs.est.5b03355 Google Scholar

39. Zheng, W.; Obrist, D.; Weis, D.; Bergquist, B. A. Mercury isotope compositions across North American forests. *Glob. Biogeochem. Cycles* **2016**, *30*, 1475– 1492, DOI: 10.1002/2015GB005323 Google Scholar

40. Bergquist, B. A.; Blum, J. D. Mass-dependent and -independent fractionation of Hg isotopes by photoreduction in aquatic systems. *Science* **2007**, *318*, 417– 420, DOI: 10.1126/science.1148050 Google Scholar

41. Jiskra, M.; Wiederhold, J. G.; Skyllberg, U.; Kronberg, R. M.; Hajdas, I.; Kretzschmar, R. Mercury deposition and re-emission pathways in boreal forest soils investigated with Hg isotope signatures. *Environ. Sci. Technol.* **2015**, *49*, 7188– 7196, DOI: 10.1021/acs.est.5b00742 Google Scholar

42. Korpiel, J. A.; Vidic, R. D. Effect of sulfur impregnation method on activated carbon uptake of gas-phase mercury. *Environ. Sci. Technol.* **1997**, *31*, 2319– 2325, DOI: 10.1021/es9609260 Google Scholar

43. Diamantopoulou, I.; Skodras, G.; Sakellaropoulos, G. P. Sorption of mercury by activated carbon in the presence of flue gas components. *Fuel Process. Technol.* **2010**, *91*, 158– 163, DOI: 10.1016/j.fuproc.2009.09.005 Google Scholar

44. Huang, C. P.; Blankenship, D. W. The removal of mercury(II) from dilute aqueous solution by activated carbon. *Water Res.* **1984**, *18*, 37– 46, DOI: 10.1016/0043-1354(84)90045-9 Google Scholar

45. Balogh, S. J.; Huang, Y.; Offerman, H. J.; Meyer, M. L.; Johnson, D. K. Episodes of elevated methylmercury concentrations in prairie streams. *Environ. Sci. Technol.* **2002**, *36*, 1665– 1670, DOI: 10.1021/es011265w Google Scholar

46. Riggs, C. E.; Kolka, R. K.; Nater, E. A.; Witt, E. L.; Wickman, T. R.; Woodruff, L. G.; Butcher, J. T. Yellow perch (*Perca flavescens*) mercury unaffected by wildland fires in northern Minnesota. *J. Environ. Qual.* **2017**, *46*, 623– 631, DOI: 10.2134/jeq2016.10.0418 Google Scholar

47. Gratz, L. E.; Keeler, G. J.; Blum, J. D.; Sherman, L. S. Isotopic composition and fractionation of mercury in Great Lakes precipitation and ambient air. *Environ. Sci. Technol.* **2010**, *44*, 7764– 7770, DOI: 10.1021/es100383w Google Scholar

48. Sherman, L. S.; Blum, J. D.; Johnson, K. P.; Keeler, G. J.; Barres, J. A.; Douglas, T. A. Mass-independent fractionation of mercury isotopes in Arctic snow driven by sunlight. *Nat. Geosci.* **2010**, *3*, 173– 177, DOI: 10.1038/ngeo758 Google Scholar

49. Demers, J. D.; Blum, J. D.; Zak, D. R. Mercury isotopes in a forested ecosystem: Implications for air-surface exchange dynamics and the global mercury cycle. *Glob. Biogeochem. Cycles* **2013**, *27*, 222– 238, DOI: 10.1002/gbc.20021 Google Scholar

Supporting Information (SI)

Origin, reactivity, and bioavailability of mercury in wildfire ash

Peijia Ku [†], Martin Tsz-Ki Tsui [†], Xiangping Nie [ζ], Huan Chen [§], Tham C. Hoang [¶], Joel D. Blum [#], Randy A. Dahlgren [‖], Alex T. Chow [§]

[†] *Department of Biology, University of North Carolina at Greensboro, Greensboro, North Carolina 27402*
[ζ] *Department of Ecology, Jinan University, Guangzhou, 510632, China*
[§] *Biogeochemistry & Environmental Quality Research Group, Clemson University, Georgetown, South Carolina 29442*
[¶] *Institute of Environmental Sustainability, Loyola University Chicago, Chicago, Illinois 60660*
[#] *Department of Earth and Environmental Sciences, University of Michigan, Ann Arbor, Michigan 48109*
[‖] *Department of Land, Air and Water Resources, University of California, Davis, California 95616*

Summary of content

no. of pages: 23
no. of text: 6
no. of tables: 7
no. of figures: 7

SI Text 1 – Physiochemical measurements and Py-GC/MS analysis

Loss-on-ignition (LOI) for all samples was measured after being held in a muffle furnace (Thermo Scientific; Thermolyne™) at 500 °C for 4 hours at the University of North Carolina at Greensboro (UNCG; Greensboro, NC). Total carbon (TC) and total nitrogen (TN) contents were analyzed on a CHN-O elemental analyzer (Thermo Scientific; FLASH 2000) at Baruch Institute of Coastal Ecology, Clemson University (Georgetown, SC). Major cations and trace elements were also analyzed for samples after acid digestion (aqua regia; following Olund et al.)[1] and dilution with Barnstead™ Nanopure™ water (18.2 MΩ/cm) using inductively coupled plasma–mass spectrometry (Perkin Elmer; NeXion 300S) at Institute of Environmental Sustainability, Loyola University Chicago (Chicago, IL).

The organic carbon composition in ash and unburned samples was determined by pyrolysis-gas chromatography-mass spectrometry (Py-GC-MS) at Baruch Institute of Coastal Ecology, Clemson University, following a method described by Song and Peng[2] and Chen et al.[3] In brief, individual samples (0.1-30 mg depending on organic matter content) were placed in pre-baked quartz tubes with samples held in place by glass wool. The sample-filled quartz tube was introduced into the CDS Analytical Pyroprobe 2000 "Pyrolyzer" and heated from 250 to 700 ºC with a temperature ramping rate of 5 ºC/millisecond and then held for 10 s on a pyrolysis injector (CDS Analytical Inc., Oxford, PA) connected to a gas chromatography-mass spectrometer (GC-MS; Agilent 7890A). Helium gas at 1 mL/min was used to flush the pyrolytic compounds into the GC column. The GC injector was operated in split-mode (10:1 to 50:1 depending on the organic matter content in sample) with an inlet temperature of 250 ºC. Pyrolysis products were identified and quantified according to their GC retention time and mass spectra with reference to the Wiley/NIST library supplied with the MS workstation software 7.0.1.

The identified and quantified pyrolysis products were classified into nine groups according to their chemical similarity: (*i*) saturated hydrocarbon (SaH), (*ii*) unsaturated hydrocarbon (UnSaH), (*iii*) aromatic hydrocarbon (ArH), (*iv*) polyaromatic hydrocarbon (PAH), (*v*) carbohydrate (Carb), (*vi*) phenolic carbohydrate (PhC), (*vii*) lignin phenol carbohydrate (LgPhC), (*viii*) halogen-containing compounds (Hal), and (*ix*) nitrogen-containing compounds (Ntg). Relative abundance of each group was calculated as the sum of the major ion peak areas in each group divided by the sum of all major ion peak areas. An R-script (R Studio Desktop version 1.0.44; Boston, MA) was developed for automated identification and quantification.

SI Text 2 – Sample digestion and Hg analysis

All sample processing and analysis for Hg was performed in a semi-clean analytical laboratory at UNCG. For all samples, we used two acid digestion methods to release Hg in order to assess Hg reactivity based on the differences of Hg concentrations generated by the two digestion methods. In *Method 1* (reported as [$Hg_{method-1}$]), 0.20±0.01 g of dry samples were weighed into acid-cleaned PFA digestion vessels (Savillex, Eden Prairie, MN), and 5 mL of trace-metal grade HNO_3 and H_2O_2 (4:1, v:v, both from Fisher Scientific) were added and allowed to sit at room temperature overnight with the cap loosely tightened (i.e., cold digestion). On the following day, the digestion vessels were tightly closed and placed in a water bath at 80 ^oC overnight to complete the digestion (i.e., hot digestion). *Method 2* (reported as [$Hg_{method-2}$]) followed the procedure of Olund et al.[1] in which samples were weighed into acid-cleaned 40 mL borosilicate glass vials with PTFE-lined septa (Thermo Scientific), and 8 mL of trace-metal grade HNO_3 and HCl (i.e., aqua regia; 1:3, v:v, both from Fisher Scientific) was added and allowed to sit at room temperature for 24 h (i.e., cold digestion). Then, 22 mL of 5% BrCl was added to the acidic mixtures, and the vials containing sample mixtures were placed in a water bath at 80 ^oC overnight (i.e., hot digestion). To test the robustness of this approach to assess Hg reactivity in environmental samples, we also analyzed two vegetation standard reference materials (SRMs) (i.e., NIST-1515 Apple Leaves; IAEA-359 Cabbage) and litter samples from three reference forests (Angelo Coast Range Reserve in northern California, University of Michigan Biological Station in northern Michigan, and Hubbard Brook Experimental Forest in New Hampshire).

For both digestion methods, aliquots of digested samples (0.5 to 2 mL, depending on estimated Hg content) were added to 100 mL of Nanopure water (18.2 MΩ/cm) in a glass bubbler with stopper/sparger and 200-600 µL of 30% hydroxylamine (Alfa Aesar) were added to partially reduce the reagent. Gold traps were attached in connection to a soda lime trap to collect gaseous Hg(0) following complete reduction by 200 µL of 20% stannous chloride (Alfa Aesar), and the mixture was purged with Hg-free N_2 gas for 15 minutes. Gold traps loaded with Hg were heat-desorbed at 400-500 ^oC using the double amalgamation technique, and sample Hg was quantified using a Brooks Rand Model III CVAFS detector.

Throughout sample analyses, random samples were digested in duplicate and run for Hg. A primary calibration standard solution (1 ng/mL) was prepared from SMR-NIST-3133 Hg solution and checked against an in-house secondary calibration standard (1 ng/mL) prepared from SRM-NIST-1641d Hg solution; Hg in the two standards always matched within 3%. For each batch of digestions using both methods, we included reagent blanks and standard reference materials (SRM-NIST-1515 Apple Leaves and SRM-IAEA-

359 Cabbage). Hg results were not significantly different (p>0.05) based on the two digestion methods for SRM-NIST-1515: [$Hg_{method-1}$] was 42.3±0.99 ng/g (n=7; mean±s.d.) and [$Hg_{method-2}$] was 45.1±2.19 ng/g (n=9) (**Table S3**), while the certified value for SRM-NIST-1515 had a mean of 44.0 ng/g (range = 40.0-48.0 ng/g). Similarly, Hg results were not significantly different (p>0.05) based on the two digestion methods for SRM-IAEA-359: [$Hg_{method-1}$] was 10.2±0.88 ng/g (n=3) and [$Hg_{method-2}$] was 10.8±1.29 ng/g (n=3) (**Table S3**). The certified value for SRM-IAEA-359 has a mean of 13.0 ng/g (range = 11.0-15.0 ng/g). All digested reagent blank had Hg concentrations <1 ng/g (based on the same procedure as in method 2).

SI Text 3 – Estimation of Hg volatilization in ash samples

We estimated the Hg volatilization percentage for each ash sample collected in the field. We assumed the wildfire ash was generated from the combustion of the unburned vegetation components (litter and wood) from each site. We used two mass balance methods to calculate Hg volatilization loss based on either LOI or calcium content of ash samples.

Using LOI of the ash, we assumed that the mineral components in the ash samples were completely "conserved" during combustion from the original vegetation materials. We found that the average LOI of unburned vegetation was 95.9%, which means that 4.1% of the original vegetation materials was retained in the BA and WA samples after wildfire/combustion. Therefore, we calculated the amount of biomass combusted to form the ash mineral component (total sample weight – loss on ignition) (Mineral content % = 100% - LOI%), using the equation $\%Hg\ volatilized = 1 - Hg_{ash} / [(1\text{-}LOI_{ash}\%)/(1\text{-}LOI_{unburned}\%) \times Hg_{unburned}] \times 100\%$, in which the average $LOI_{unburned}$ % was 95.7% for Wragg Fire, and 96.0% for Rocky Fire and the average $Hg_{unburned}$ was 26.8 ng/g for Wragg Fire and 21.2 ng/g for Rocky Fire site (LOI and Hg data are shown in **SI Table S2**)

Using Ca content of the ash, we assumed no change in Ca content in the original vegetation of the wildfire conditions (i.e., no loss of Ca). We used this equation: $\%Hg\ volatilized = 1 - Hg_{ash} / [(1\text{-}Ca_{ash}\%)/(1\text{-}Ca_{unburned}\%) \times Hg_{unburned}] \times 100\%$, in which the average Ca content of unburned vegetation was 14.7 mg/g for Wragg Fire site and 10.5 mg/g for Rocky Fire site, and the average $Hg_{unburned}$ concentration was 26.8 ng/g for Wragg Fire site and 21.2 ng/g for Rocky Fire site (Ca and Hg data are shown in **SI Table S2**).

SI Text 4 – Sample processing and stable Hg isotope analysis

We performed thermal combustion for stable Hg isotope analysis on unburned litter from three natural,

unburned forests in the U.S. (Angelo Coast Range Reserve in northern California, University of Michigan Biological Station in northern Michigan, and Hubbard Brook Experimental Forest in central New Hampshire) and the Wragg Fire ash samples (*n*=10; 5 black ash [BA] and 5 white ash [WA]). Prior to thermal combustion, each dry sample was weighed into two clean ceramic sample boats (~0.5-1.0 g per boat), and packed with layers of pre-baked combustion powders (Nippon Instruments Corporation). Samples with low Hg content required multiple rounds of combustion and sample Hg was later combined during the purge-and-trap sample purification step in order to have sufficient Hg (> 10 ng) for high-precision isotopic analysis (*see below*).

In brief, samples were thermally combusted in a two-stage furnace (the first furnace ramped from room temperature to 750 ^{o}C over 6 hours and the second furnace was held at 1,000 ^{o}C for the entire period). The released gaseous Hg(0) was collected into a 24 g trap solution containing 1% $KMnO_4$ (w/w) in 10% trace-metal grade H_2SO_4 (v/v). Following combustion, the trap solution was transferred into an acid-cleaned 40 mL borosilicate glass vial with PTFE-lined septum. To analyze Hg content, the trap solution was completely neutralized with 30% hydroxylamine, and an aliquot of solution was taken for quantification of Hg using the CVAFS system (Brooks Rand Model III CVAFS; described in **SI Text 2**).

Mercury in the initial trap solution (from combustion) was purged (upon complete reduction by 20% $SnCl_2$) and trapped into a smaller trap solution (6 to 15 g of 1% $KMnO_4$ in 10% H_2SO_4, depending on the total amount of sample Hg) in order to (*i*) separate sample Hg from other combustion products in the initial trap solution, and (*ii*) concentrate Hg in this final solution for Hg isotope analysis. The final trap solution was neutralized and an aliquot of solution was taken for analyzing Hg to determine the recovery of Hg during the purge-and-trap (typically > 95%). Hg levels in the final trap solution were precisely adjusted to a uniform Hg concentration (± 5%) along with a bracketing Hg isotope standard (SRM-NIST-3133) ranging from 2-5 ng/g (Blum and Bergquist, 2007).

Stable Hg isotope ratios were measured using a Nu Instruments multicollector-inductively coupled plasma-mass spectrometer (MC-ICP-MS) following the methods of Blum and Bergquist[4] in the Biogeochemistry and Environmental Isotope Geochemistry Laboratory at the University of Michigan (Ann Arbor, MI). Mass-dependent fractionation (MDF) of Hg isotopes was reported as δ^{202}Hg in permil (‰) referenced to SRM-NIST-3133, while mass-independent fractionation (MIF) of Hg isotopes is the difference between the measured δ^{202}Hg value and the value that would be predicted based on mass dependence. The mass-independent Hg isotope composition is reported in ‰ for both odd-mass isotopes Δ^{199}Hg and Δ^{201}Hg and even-mass isotopes Δ^{200}Hg and Δ^{204}Hg. Isotopic compositions were calculated

according to Blum and Bergquist[4] as:

$$\delta^{202}Hg = \{[(^{202}Hg / {}^{198}Hg)_{sample} \div (^{202}Hg / {}^{198}Hg)_{NIST\ 3133}] - 1\} \times 1000 \quad (1)$$

$$\Delta^{201}Hg \approx \delta^{201}Hg_{measured} - (\delta^{202}Hg_{measured} \times 0.752) \quad (2)$$

$$\Delta^{199}Hg \approx \delta^{199}Hg_{measured} - (\delta^{202}Hg_{measured} \times 0.2520) \quad (3)$$

$$\Delta^{200}Hg \approx \delta^{200}Hg_{measured} - (\delta^{202}Hg_{measured} \times 0.5024) \quad (4)$$

$$\Delta^{204}Hg \approx \delta^{204}Hg_{measured} - (\delta^{202}Hg_{measured} \times 1.4930) \quad (5)$$

Analytical uncertainty was determined from replicated analyses of a secondary standard solution (UM-Almadén, mean values: $\delta^{202}Hg$ = -0.56 ‰; $\Delta^{199}Hg$ = -0.02 ‰; *n*=11), and replicate combustions and analyses of SRM-NIST-1515 (Apple Leaves [UNCG lot], mean values: $\delta^{202}Hg$ = -2.64 ‰; $\Delta^{199}Hg$ = 0.05 ‰; *n*=6) along with the field samples. These isotopic compositions are similar to previous studies (e.g., Demers et al.)[5]. External analytical reproducibility of $\delta^{202}Hg$ measurements was estimated to be ±0.08‰ for solutions with 5.0 ng/g and ±0.14 ‰ for 1.9 ng/g (2 SD) and for $\Delta^{199}Hg$ it was estimated to be ±0.07 ‰ (2 SD), based on the repeated analyses of SRM-NRCC-TORT-2 analyzed at different final Hg concentrations on MC-ICP-MS (1.9-5.0 ng/g).[6,7]

SI Text 5 – Testing sorption capability of Hg by wildfire ash

The ability of wildfire ash to adsorb aqueous Hg(II) was assessed in two sorption experiments that involved adding 1.0 g of ash (4 black ash and 4 white ash from the Wragg Fire, and activated carbon [CAS 7440-44-0; Alfa Aesar] as a positive control) into 100 mL of 18.2 MΩ/cm water spiked with $HgCl_2$ (Sigma-Aldrich) in 500 mL acid-cleaned borosilicate glass Erlenmeyer flasks. The mean actual Hg concentration in filtered, spiked solution before sorption was 70.3 pg/mL in the first experiment and 74.8 pg/mL in the second experiment. The ash as a solid slurry was shaken for 24 h on a shaker table at room temperature. The slurry was filtered through a pre-baked glass fiber filter (Whatman GF/B, 1.0-µm pore size). Filtered aqueous samples were treated with an acidic mixture of permanganate/persulfate and heated at 80 °C overnight to complete sample digestion.[8] Digested samples were neutralized, and weighed aliquots were analyzed for Hg as previously described.

To test the capability of ash at adsorbing gaseous elemental Hg(0), we set up a sorption experiment using the purge-and-trap setup we routinely used for purging large volumes of stream water for Hg isotopic analysis (*see setup and detailed procedures in* Woerndle et al.)[8]. The Hg(0) gas is slowly released by this method as $SnCl_2$ is slowly added to the reservoir of aqueous sample with Hg, as opposed to the situation

for Hg analysis described above. In brief, we prepared 500 mL of acidic solution spiked with 15.0 ng of Hg from our SRM-NIST-3133 standard solution. We purged this solution by adding 10% $SnCl_2$ at a rate of ~1 mL/min. Reduced Hg(0) was sparged with 0.45-μm filtered Hg-free ambient air (produced by a vacuum pump and passed through a Teflon filter and a gold-coated glass trap), and transferred through a soda lime trap (to remove moisture and neutralize acidic fumes) and a Teflon trap with only glass wool (as a negative control) or filled with an ash sample (Wragg Fire BA and WA) or activated carbon (CAS 7440-44-0; Alfa Aesar) as a positive control. The length of packed material inside the Teflon trap was 4.2 cm with an average mass of materials of 1.22±0.14 g (mean±s.d.). Any Hg(0) not removed by the ash or activated carbon trap was collected by the final, downstream gold trap. The gold trap was dried with Hg-free N_2 gas for 20 minutes, and analyzed for Hg as described above.

SI Text 6 – Examining bioavailability of Hg in ash during incubation

We conducted 4- and 12-week incubation experiments of ash and an unburned litter sample from a northern California forest (Angelo Coast Range Reserve, Branscomb, CA) using sealed bottles. Previous studies have demonstrated that sealed bottle incubation with fresh litter and freshly collected stream water quickly turned anoxic (<1 week) and active microbial Hg methylation quickly proceeded with inorganic Hg(II) released from the decomposing litter.[9,10] This study inoculated samples with the microbial community in freshly collected surface water from an urban stream near UNCG (South Buffalo Creek at Greensboro, NC; GPS location: 36.050563, -79.748731). A preliminary experiment using "aged" stream water (>3 months stored at 4 ^oC) from the catchment burned by the Wragg Fire in California did not result in detectable levels of MeHg even in the litter-incubated treatment (*data not shown*). This suggests that the anaerobic, methylating microbes needed to be derived from water freshly collected from the ambient environment.

In brief, the incubation experiments used 250 mL air-tight, sterile PETG bottles (Nalgene), and each bottle received 2.80±0.01 g of 2-mm sieved ash or homogenized litter sample. A 280±1.21 mL of unfiltered stream water (with resultant minimal head space in the container) was added to achieve a solid-to-water ratio of 10 g/L, which was 5 times higher than our previous incubation experiments using similar methods.[10] The bottle was tightly capped and further wrapped with layers of Parafilm to secure the closing. We did not flush the ash slurry with N_2 gas as anoxia was expected to develop quickly over the course of incubation. Each treatment was performed in triplicate. Sealed bottles were placed in the dark at room temperature (20-22 ^oC) for 4 weeks or 12 weeks. Each bottle was shaken daily to mix the contents.[10,11]

At the end of the incubation, bottles were opened and the "rotten egg" odor (i.e., hydrogen sulfide) was noted if it was present or absent to indicate the existence of sulfate-reduction during incubation.[9,10] The aqueous solution was immediately filtered through a pre-baked Whatman GF/B filter (1.0-µm pore size) in an acid- and BrCl-cleaned glass filtration apparatus (Kimble™ Kontes™). Filtered samples were analyzed separately for pH, specific conductivity (12-week samples only), total-dissolved nitrogen (TDN), dissolved organic carbon (DOC), $SUVA_{254}$ (proxy for aromaticity of DOC), Hg and methylmercury (MeHg).

Hg in filtered water samples was analyzed after digestion using an acidic mixture of $KMnO_4$ and $K_2S_2O_8$, and heated at 80 ^oC overnight.[8] Filtered water samples were preserved with 0.4 % HCl[12] and kept in the dark at 4 ^oC prior to distillation for matrix removal and MeHg analysis (Brooks Rand Model III CVAFS with GC/pyrolysis module). Procedures for MeHg analysis in aqueous samples at the UNCG laboratory are fully described in Woerndle et al.[8] Percent of Hg as MeHg (i.e., %MeHg) in the filtered solution was used to evaluate Hg methylation potential, or conversely, the bioavailability of Hg for microbial methylation.[10,13]

Measured physiochemical properties of the filtered solution included pH (Mettler Toledo pH meter), specific conductivity (Fisher Scientific conductivity meter), dissolved organic carbon (DOC) and total-dissolved nitrogen (TDN) (Shimadzu TOC analyzer). The UV-absorbance at 254 nm (UV_{254}) was measured using a diode array spectrophotometer (Hewlett Packard P8452A) and then used to calculate specific UV absorbance at 254 nm ($SUVA_{254}$; in L/mg-C/m) as a proxy for DOC aromaticity.[14]

223 **Table S1** Summary of wildfire site characteristics and sampling information.

	Wragg Fire	**Rocky Fire**
Dates	July 22 to August 5, 2015	July 29 to August 14, 2015
Locations	Lake Berryessa, CA	Clearlake, CA
Coordinates	38°29'12.98"N, 122° 4'30.29"W	38°57'48.29"N, 122°29'10.91"W
Burned area	33 km^2	281 km^2
Soil parent material	Mixed sedimentary: shale, mudstone & sandstone	Mixed sedimentary: shale, mudstone & sandstone
Dominant soils	Lithic Haploxerepts & Typic Dystroxerepts	Typic Dystroxerepts *& Mollic Haploxeralfs*
Dominant vegetation	Blue oak, live oak, scrub oak, chamise, manzanita, ceonothus	Blue oak, live oak, scrub oak, chamise, manzanita, ceonothus
Date of sampling	August 25, 2015	September 19, 2015
Rainfall prior to sampling	No	No
Sampling points	*~ 0.5 km transect / trail*	*~ 10-11 km between sites, along fire perimeter*
	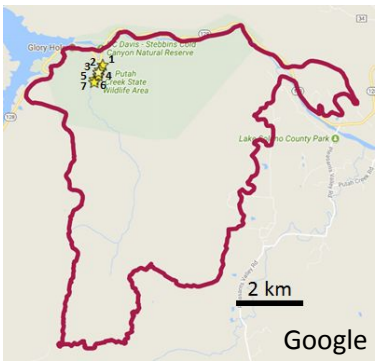	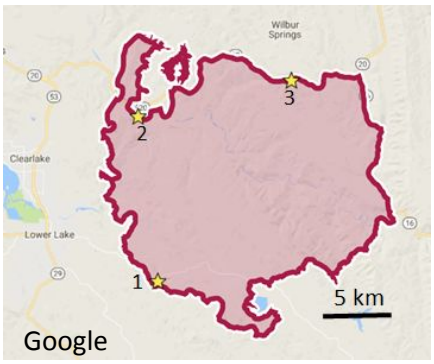
	WR1: 1xWA, 1xBA WR2: 1xWA WR3: 1xWA, 1xBA WR4: 1xBA WR5: 1xBA WR6: 1xWA WR7: 1XWA, 1xBA	RO1: 3xWA, 3xBA RO2: 3xWA, 3xBA RO3: 3xWA, 3xBA

224

Table S2 Different physicochemical properties of standard reference materials (SRMs), litter samples from reference forests, ash and unburned samples from the Wragg Fire (2015), and ash and unburned samples from the Rocky Fire (2015). *Note:* SRM-NIST-1515: apple leaves (*n*=9); SRM-IAEA-359: cabbage (*n*=3); CA-Litter: Angelo Coast Range Reserve (*n*=1); NH-Litter: Hubbard Brook Experimental Forest (*n*=3); MI-Litter: University of Michigan Biological Station (*n*=3). Individual sample data are shown for all ash and unburned samples. ND = not determined.

Category	Sample ID	Munsell color (Hue Value/Chroma)	LOI (%)	TN (%)	Ca (%)	Fe (%)	$Hg_{method-1}$ (ng/g)	$Hg_{method-2}$ (ng/g)	Recalcitrant Hg (%)	Relative abundance of pyrolysis products (%)								
										SaH	UnSaH	ArH	PAH	Carb	PhC	LgPhC	Hal	Ntg
SRMs	NIST-1515	ND	ND	ND	1.7	0.012	42.3	45.1	8.7	ND	ND	ND	ND	ND	ND	ND	ND	ND
	IAEA-359	ND	ND	ND	1.7	0.020	10.2	10.8	6.1	ND	ND	ND	ND	ND	ND	ND	ND	ND
Litter (ref. forests)	CA-Litter	ND	93.7	0.69	2.0	0.048	32.2	35.0	8.2	0	2	13	0	20	50	16	0	0
	NH-Litter	ND	96.3	1.73	ND	ND	53.2	57.8	8.2	4	19	8	4	21	23	17	1	6
	MI-Litter	ND	97.1	0.90	ND	ND	41.7	45.0	7.3	4	19	9	4	21	24	16	0	5
Wragg-unburned	Oak Litter	ND	94.8	1.97	1.4	0.80	27.2	28.1	3.1	1	0	11	0	36	13	8	0	30
	Pine Litter	ND	96.3	1.39	1.0	0.14	42.6	40.1	0	1	0	12	1	33	22	10	1	19
	Oak Wood	ND	92.7	0.69	3.1	0.04	25.4	24.3	4.6	1	1	6	0	25	11	15	0	41
	Pine Wood	ND	98.6	0.44	0.4	0.02	14.1	14.6	3.5	0	0	5	0	21	26	16	5	31
Wragg-black ash	WR1-BA	Gley1 3.5/N	31.0	0.64	9.7	2.3	2.8	7.9	64.7	3	4	61	2	7	5	0	2	15
	WR3-BA	Gley1 3/N	35.8	1.39	6.4	2.7	9.8	18.1	46.1	5	5	31	1	16	20	6	3	12
	WR4-BA	Gley 1 3.5/N	23.2	1.08	6.1	2.8	7.8	12.2	35.7	7	7	36	1	16	13	1	4	15
	WR5-BA	ND	49.3	1.54	9.3	1.4	9.7	10.6	7.9	9	33	17	2	6	26	2	0	6
	WR7-BA	Gley 1 2.75/N	36.9	1.17	6.0	2.9	8.1	10.7	24.5	7	38	15	3	4	14	0	0	20
Wragg-white ash	WR1-WA	Gley1 5.5/N	6.6	0.23	24.9	1.7	8.6	9.2	6.2	7	30	33	3	6	2	0	3	15
	WR2-WA	Gley1 7/N	2.9	0.11	29.0	1.4	15.6	16.4	4.9	0	0	80	5	1	0	0	0	14
	WR3-WA	Gley1 5.5/N	4.0	0.14	26.2	2.1	15.0	14.8	0	0	1	77	5	3	0	0	0	13
	WR6-WA	Gley1 5.5/N	4.0	0.15	30.1	1.6	119.8	124.6	3.9	0	3	74	6	4	0	0	0	14
	WR7-WA	Gley1 5.5/N	5.9	0.17	28.0	1.3	7.5	8.8	14.3	2	12	62	6	1	0	0	0	17
Rocky-unburned	Oak Litter	ND	94.0	1.87	1.3	0.02	18.3	20.3	9.5	1	0	16	0	34	24	6	0	20
	Pine Litter	ND	97.4	0.62	0.7	0.01	28.4	30.1	5.8	0	0	12	2	33	26	8	1	19
	Oak Wood	ND	95.9	0.67	1.8	0.02	16.0	16.2	1.1	1	0	4	0	15	8	24	0	49
	Pine Wood	ND	98.6	0.55	0.6	0.01	73.3	57.0	0.0	0	0	5	0	17	39	15	0	24
Rocky-black ash	RO1-BA1	Gley1 2.5/N	26.9	0.60	5.1	4.8	7.2	26.5	72.7	2	5	52	3	8	18	1	1	9
	RO1-BA2	Gley1 2.5/N	31.2	0.40	2.9	5.2	12.8	31.8	59.8	5	11	47	2	14	13	3	1	4
	RO1-BA3	Gley1 2.75/N	33.6	0.45	4.4	5.2	14.1	56.5	75.1	4	10	47	3	10	12	3	2	9
	RO2-BA1	Gley1 2.5/N	58.3	2.06	4.2	1.8	28.3	42.6	33.6	4	7	35	2	15	19	2	2	13
	RO2-BA2	10YR 2/1	62.1	2.11	3.1	1.2	8.9	15.8	43.4	4	6	39	3	12	16	5	2	14
	RO2-BA3	Gley1 2.5/N	44.0	1.54	3.1	2.6	27.4	48.2	43.2	4	7	29	1	14	21	9	2	12
	RO3-BA1	10YR 2/1	38.0	1.00	4.8	3.4	47.8	94.0	49.2	3	6	45	4	12	18	1	2	11
	RO3-BA2	2.5Y 2.5/1	60.9	1.85	4.2	1.8	29.0	42.9	32.3	4	5	29	1	16	21	11	1	11
	RO3-BA3	5Y 2.5/1	52.3	1.40	3.4	2.3	27.1	39.9	32.0	4	5	29	1	18	21	8	3	12
Rocky-white ash	RO1-WA1	10YR 7.5/1	2.4	0.08	26.5	2.3	40.4	78.0	48.2	0	1	86	4	3	0	0	0	7
	RO1-WA2	10YR 7/1	2.6	0.09	26.8	2.3	11.6	13.9	16.6	0	0	83	5	3	0	0	0	10
	RO1-WA3	2.5Y 7/1	5.5	0.16	27.5	2.1	42.0	61.8	32.1	3	5	58	5	13	1	0	0	16
	RO2-WA1	2.5Y 6.5/1	15.2	0.06	15.9	1.4	4.0	5.9	31.7	6	7	69	4	9	1	0	0	5
	RO2-WA2	Gley1 7.5/N	3.0	0.07	34.0	1.5	30.8	32.4	5.1	2	4	72	7	7	1	0	0	7
	RO2-WA3	WP 8.75/N	2.9	0.00	36.5	1.1	1.7	3.9	56.1	6	16	51	3	22	0	0	0	2
	RO3-WA1	2.5Y 7.5/1	7.8	0.00	33.9	1.0	2.9	5.0	41.8	2	5	68	7	5	0	0	0	14
	RO3-WA2	2.5Y 6/1	3.7	0.07	43.2	0.6	12.4	14.0	11.3	7	10	58	4	12	3	0	2	3
	RO3-WA3	Gley1 7.5/N	3.4	0.05	30.2	1.4	5.8	8.4	30.7	3	5	69	6	7	0	0	0	10

Table S3 Estimated mercury (Hg) volatilization from original fuel loads (assumed to be a mixture of litter and dead woody materials) in the Wragg Fire (2015; WR) and the Rocky Fire (2015l RO). Our estimations are based on two approaches: loss-on-ignition (LOI) and calcium (Ca) content of ash samples.

Sample ID	Hg volatilization (%) *based on LOI*	Hg volatilization (%) *based on Ca content*
WR1-BA	98.6	96.3
WR3-BA	96.6	87.1
WR4-BA	98.1	90.9
WR5-BA	97.5	94.8
WR7-BA	98.0	91.9
WR1-WA	99.2	98.2
WR2-WA	98.6	97.3
WR3-WA	98.7	97.3
WR6-WA	89.3	80.1
WR7-WA	99.2	98.5
RO1-BA1	91.7	82.6
RO1-BA2	89.4	62.8
RO1-BA3	80.4	56.6
RO2-BA1	76.5	66.2
RO2-BA2	90.4	82.8
RO2-BA3	80.2	47.2
RO3-BA1	65.1	34.0
RO3-BA2	74.7	65.4
RO3-BA3	80.7	60.5
RO1-WA1	81.6	90.1
RO1-WA2	96.7	98.3
RO1-WA3	84.9	92.4
RO2-WA1	98.4	98.8
RO2-WA2	92.3	96.8
RO2-WA3	99.1	99.6
RO3-WA1	98.7	99.5
RO3-WA2	96.6	98.9
RO3-WA3	98.0	99.1

Table S4 Stable mercury (Hg) isotope compositions of undecomposed litter from reference forests, published data on foliage in other North American forests[15], and black ash (BA) and white ash (WA) samples from Wragg Fire (2015). *Note:* MDF=mass dependent fractionation; MIF=mass independent fractionation.

Sample type and/or sources	Location / Sample ID	δ^{202}Hg (‰) [MDF]	Δ^{204}Hg (‰) [MIF]	Δ^{201}Hg (‰) [MIF]	Δ^{200}Hg (‰) [MIF]	Δ^{199}Hg (‰) [MIF]
Reference forests	Angelo Forest / CA-Litter	-2.07	0.12	-0.37	-0.04	-0.43
	Hubbard Forest / HB-Litter 1	-1.98	0.01	-0.38	0.03	-0.39
	Hubbard Forest / HB-Litter 2	-2.16	0.00	-0.34	-0.01	-0.38
	Hubbard Forest / HB-Litter 3	-2.10	0.02	-0.28	0.01	-0.32
	U-M Biostation / MI-Litter 1	-2.03	-0.01	-0.30	0.00	-0.32
	U-M Biostation / MI-Litter 2	-2.11	0.05	-0.21	-0.04	-0.22
	U-M Biostation / MI-Litter 3	-2.05	0.03	-0.22	0.00	-0.24
Published data in foliage in other North American forests (Zheng et al.)[15]	Truckee, CA	-2.67	-0.01	-0.04	0.01	-0.10
		-2.27	0.01	-0.04	0.04	-0.06
		-2.08	-0.01	0.00	0.02	-0.06
	Niwot Ridge, CO	-2.31	-0.01	-0.31	-0.04	-0.35
		-2.32	0.01	-0.18	0.00	-0.20
	Howland, ME	-2.35	0.08	-0.24	-0.05	-0.30
		-2.38	0.06	-0.27	-0.02	-0.30
	Thompson Forest, WA	-2.66	0.00	-0.47	0.01	-0.47
		-2.45	0.02	-0.35	-0.01	-0.36
Black ash (BA)	WR1-BA	-1.87	-0.01	-0.20	0.08	-0.17
	WR3-BA	-1.65	-0.03	-0.20	0.03	-0.14
	WR4-BA	-1.60	-0.05	-0.13	0.03	-0.04
	WR5-BA	-1.46	0.09	-0.19	0.01	-0.21
	WR7-BA	-2.14	0.00	-0.03	0.01	0.10
White ash (WA)	WR1-WA	-1.93	-0.04	-0.05	0.04	-0.04
	WR2-WA	-1.05	-0.12	-0.24	-0.03	-0.16
	WR3-WA	-1.11	-0.14	0.00	-0.02	-0.02
	WR6-WA	-0.77	0.00	-0.23	0.04	-0.19
	WR7-WA	-1.62	-0.07	0.01	0.00	0.02

238 **Table S5** Summary of results from Hg in sorption experiments examining sorption of ash (from the Wragg
239 Fire only) and activated carbon on aqueous Hg(II) and gaseous Hg(0). ND = not determined.

	Removal of aqueous Hg(II) (~7.0-7.5 ng per test)	**Removal of gaseous Hg(0)** (15 ng per test)
Activated carbon	99.9%	99.9%
WR1-BA	97.2%	2.9%
WR3-BA	89.2%	1.6%
WR4-BA	95.3%	ND
WR5-BA	ND	1.4%
WR7-BA	88.3%	2.1%
WR1-WA	95.6%	ND
WR2-WA	98.3%	5.4%
WR3-WA	94.4%	0.4%
WR6-WA	ND	ND
WR7-WA	82.4%	ND

240

Table S6 Summary of results of sealed incubation experiments after 4-weeks. Results are means ± S.D., except for MeHg in which we pooled the majority of samples from replicates for analysis. All dissolved constituents represent <1.0-μm fraction. *Note:* smell is sulfide, "rotten" egg smell present (+) or absent (-); DOC=dissolved organic carbon; $SUVA_{254}$=specific ultraviolet absorbance at 254 nm (proxy of DOC aromaticity); TDN=total dissolved nitrogen; Hg=mercury; MeHg=methylmercury; %MeHg=percent of Hg as MeHg.

	Sulfidic smell	pH	DOC (mg/L)	$SUVA_{254}$ (L/mg/m)	TDN (mg/L)	Filtered Hg (ng/L)	Filtered MeHg (ng/L)	%MeHg
Water-only	-	8.0±0.0	7.6±0.2	2.0±0.1	0.9±0.0	0.7±0.1	<0.02±0.0	2.9
CA-Litter	+	5.0±0.0	277.7±3.2	1.5±0.0	7.2±0.4	11.6±0.9	0.57±0.44	4.9
WR1-BA	+	8.5±0.2	62.6±5.0	3.7±0.1	4.9±0.6	0.7±0.3	<0.02	2.9
WR3-BA	+	7.9±0.2	66.0±5.5	3.9±.1	7.1±0.6	2.3±0.2	0.22	9.6
WR4-BA	+	7.9±0.1	42.3±1.7	3.7±0.2	5.6±0.3	2.1±0.2	<0.02	1.0
WR5-BA	+	7.8±0.1	75.3±7.5	3.4±0.3	6.7±0.5	1.6±0.1	0.08	5.0
WR7-BA	+	7.9±0.1	49.3±5.4	3.5±0.1	5.5±0.5	1.7±0.2	0.19	11.2
WR1-WA	+	10.0±0.1	19.5±0.2	4.7±0.1	2.7±0.1	1.1±0.2	<0.02	1.8
WR2-WA	+	11.1±0.0	9.0±0.4	2.7±0.1	1.8±0.1	0.5±0.0	<0.02	4.0
WR3-WA	+	10.5±0.0	11.9±0.4	2.4±0.1	1.9±0.0	0.7±0.1	<0.02	2.9
WR6-WA	+	9.4±0.1	13.7±0.2	3.5±0.0	2.1±0.1	1.1±0.1	<0.02	1.8
WR7-WA	+	10.0±0.0	15.3±1.6	3.0±0.1	2.0±0.1	0.7±0.3	<0.02	2.9
RO1-BA1	+	7.6±0.0	43.8±3.1	3.6±0.3	4.3±0.1	0.7±0.1	<0.02	2.9
RO1-BA2	+	7.5±0.1	23.3±1.4	3.3±0.1	3.3±0.2	0.7±0.3	<0.02	2.9
RO1-BA3	+	7.4±0.0	42.1±6.6	2.8±0.2	3.9±0.2	0.9±0.2	<0.02	18.9
RO2-BA1	+	7.3±0.1	142.9±2.9	1.8±0.0	12.7±0.2	3.6±0.2	0.38	10.6
RO2-BA2	+	7.1±0.0	76.0±26.2	2.3±0.9	6.5±1.2	1.2±0.1	0.08	6.7
RO2-BA3	+	7.2±0.1	47.4±1.6	3.2±0.2	5.7±0.2	3.0±0.3	0.22	7.3
RO3-BA1	+	7.3±0.1	52.0±1.1	4.3±0.2	6.2±0.0	5.2±0.4	2.33±0.14	44.8
RO3-BA2	+	7.2±0.0	59.9±3.4	3.4±0.1	6.1±0.3	2.2±0.1	0.20	0.9
RO3-BA3	+	7.0±0.1	57.6±3.0	3.1±0.1	5.1±0.1	3.4±0.6	0.23	6.8
RO1-WA1	+	9.4±0.1	5.9±0.4	2.5±0.2	1.3±0.0	0.6±0.0	<0.02	3.3
RO1-WA2	+	8.9±0.2	6.4±0.3	3.0±0.2	1.5±0.1	0.7±0.2	<0.02	2.9
RO1-WA3	+	8.7±0.1	8.8±0.2	4.3±0.0	1.5±0.1	1.6±0.1	<0.02	1.3
RO2-WA1	+	10.9±0.0	7.6±0.5	1.8±0.1	1.4±0.1	0.5±0.1	<0.02	4.0
RO2-WA2	+	11.0±0.0	6.2±0.4	1.9±0.1	1.4±0.0	1.7±0.1	0.08	4.7
RO2-WA3	+	11.0±0.0	5.8±0.4	1.0±0.1	1.2±0.0	0.4±0.1	<0.02	5.0
RO3-WA1	+	10.1±0.0	5.5±0.1	2.2±0.0	1.2±0.0	0.4±0.1	<0.02	5.0
RO3-WA2	+	10.1±0.1	11.3±1.3	4.4±0.4	1.6±0.1	3.3±0.3	<0.02	0.6
RO3-WA3	+	10.2±0.0	7.1±0.7	2.5±0.2	1.4±0.1	0.6±0.1	<0.02	3.3

Table S7 Summary of results of sealed incubation experiments after 12-weeks. Results are means ± S.D., except for MeHg in which we pooled the majority of samples from replicates for analysis. All dissolved constituents represent <1.0-μm fraction. *Note:* smell is sulfide, "rotten" egg smell present (+) or absent (-); COND=conductivity; DOC=dissolved organic carbon; $SUVA_{254}$=specific ultraviolet absorbance at 254 nm (proxy of DOC aromaticity); TDN=total dissolved nitrogen; Hg=mercury; MeHg=methylmercury; %MeHg=percent of Hg as MeHg.

	Sulfidic smell	COND (μS/cm)	pH	DOC (mg/L)	$SUVA_{254}$ (L/mg/m)	TDN (mg/L)	Filtered Hg (ng/L)	Filtered MeHg (ng/L)	%MeHg
Water-only	-	124±3	6.6±0.3	7.0±0.5	2.8±0.3	0.3±0.0	0.4±0.1	<0.02	0.0
CA-Litter	+	387±4	6.8±0.4	305.6±3.6	1.5±0.1	3.6±0.5	2.8±0.2	0.13	4.8
WR1-BA	+	645±17	7.7±0.0	76.6±8.2	3.9±0.2	4.8±0.3	0.5±0.1	<0.02	3.3
WR3-BA	+	715±18	7.7±0.0	79.5±3.7	3.9±0.1	9.5±0.4	1.1±0.1	0.10	9.2
WR4-BA	+	540±38	7.8±0.0	53.1±7.8	3.7±0.2	6.5±1.1	1.3±0.1	0.06	4.4
WR5-BA	+	864±22	8.0±0.1	72.4±1.9	3.7±0.0	8.1±0.2	0.9±0.0	0.04	4.3
WR7-BA	+	607±34	7.9±0.1	57.1±3.5	3.5±0.2	6.3±0.1	1.0±0.2	0.10	10.0
WR1-WA	+	258±1	9.3±0.3	18.3±0.3	5.4±0.1	2.7±0.1	1.1±0.0	0.06	5.5
WR2-WA	+	906±86	11.2±0.1	7.9±0.3	3.5±0.2	1.7±0.1	0.6±0.1	0.04	6.9
WR3-WA	+	363±28	10.1±0.1	8.2±0.5	4.1±0.4	1.7±0.0	0.9±0.2	0.05	6.2
WR6-WA	+	432±6	9.0±0.1	8.4±0.4	5.7±0.1	2.1±0.1	0.7±0.3	0.05	6.5
WR7-WA	+	497±42	9.7±0.1	9.3±1.0	5.2±0.3	1.9±0.1	0.5±0.2	<0.02	4.3
RO1-BA1	+	493±28	8.2±0.2	37.2±3.5	5.3±0.1	4.8±0.2	0.4±0.1	0.05	11.8
RO1-BA2	+	391±29	8.0±0.1	16.3±0.5	4.4±0.1	3.0±0.1	0.4±0.0	0.03	6.7
RO1-BA3	+	422±35	7.8±0.0	29.9±1.1	4.9±0.1	3.7±0.1	0.4±0.1	0.06	13.0
RO2-BA1	+	715±23	7.8±0.1	78.8±1.3	3.4±0.0	13.8±0.3	1.6±0.1	0.05	3.1
RO2-BA2	+	641±10	7.8±0.1	56.0±0.7	3.3±0.0	7.9±0.1	0.7±0.1	0.03	4.2
RO2-BA3	+	557±5	8.0±0.2	52.6±2.6	3.4±0.1	8.8±0.3	1.6±0.2	0.05	3.3
RO3-BA1	+	598±6	7.9±0.0	54.7±1.2	4.6±0.1	8.0±0.2	1.9±0.1	0.35	18.4
RO3-BA2	+	621	8.1	52.5	3.8	8.1	1.0	0.03	3.0
RO3-BA3	+	605	8.0	53.2	3.6	7.9	1.6	0.14	8.8
RO1-WA1	+	214±3	9.0±0.0	5.0±0.2	3.0±0.0	1.1±0.1	0.5±0.1	<0.02	3.0
RO1-WA2	+	183±12	8.2±0.3	5.1±0.1	3.5±0.0	1.3±0.0	0.5±0.1	<0.02	4.7
RO1-WA3	-	306±21	8.0±0.1	7.6±0.4	4.7±0.1	1.1±0.1	1.0±0.2	<0.02	2.2
RO2-WA1	-	3,113±201	10.8±0.0	7.2±0.4	2.0±0.1	1.3±0.1	0.3±0.1	<0.02	5.0
RO2-WA2	-	948±35	11.2±0.1	6.5±0.2	2.4±0.1	1.4±0.1	5.3±1.0	0.12	2.3
RO2-WA3	+	664±50	11.1±0.1	5.0±0.2	1.4±0.1	1.0±0.0	0.3±0.1	0.04	13.6
RO3-WA1	+	1,168±42	10.0±0.0	5.1±0.1	2.4±0.1	1.0±0.1	0.4±0.1	<0.02	3.3
RO3-WA2	+	853±68	9.8±0.1	10.4±0.2	4.8±0.1	1.6±0.2	3.0±0.4	0.03	0.9
RO3-WA3	-	711±31	10.1±0.0	6.2±0.1	2.8±0.0	1.1±0.0	0.5±0.1	0.05	8.5

Fig. S1 Top-pictures of pre-sieved surface (0-5 cm depth) ash samples -- black ash (BA) and white ash (WA) from the Wragg Fire (2015). Bottom-pictures of 2-mm sieved surface (0-5 cm depth) ash samples -- black ash (BA) and white ash (WA) from the Wragg Fire (2015), and the Rocky Fire (2015). Pictures taken by P. Ku and M. Tsui.

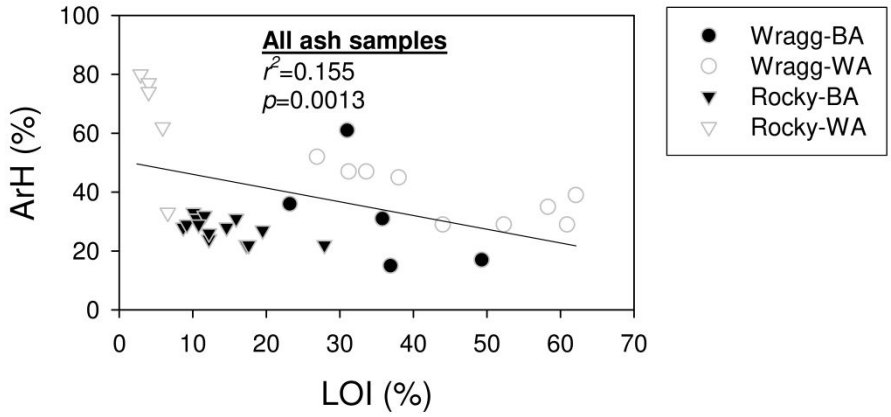

Fig. S2 Variation of percent aromatic hydrocarbon (ArH) of pyrolysis products as a function of loss-on-ignition (LOI) of black ash (BA) and white ash (WA) from the Wragg Fire and the Rocky Fire.

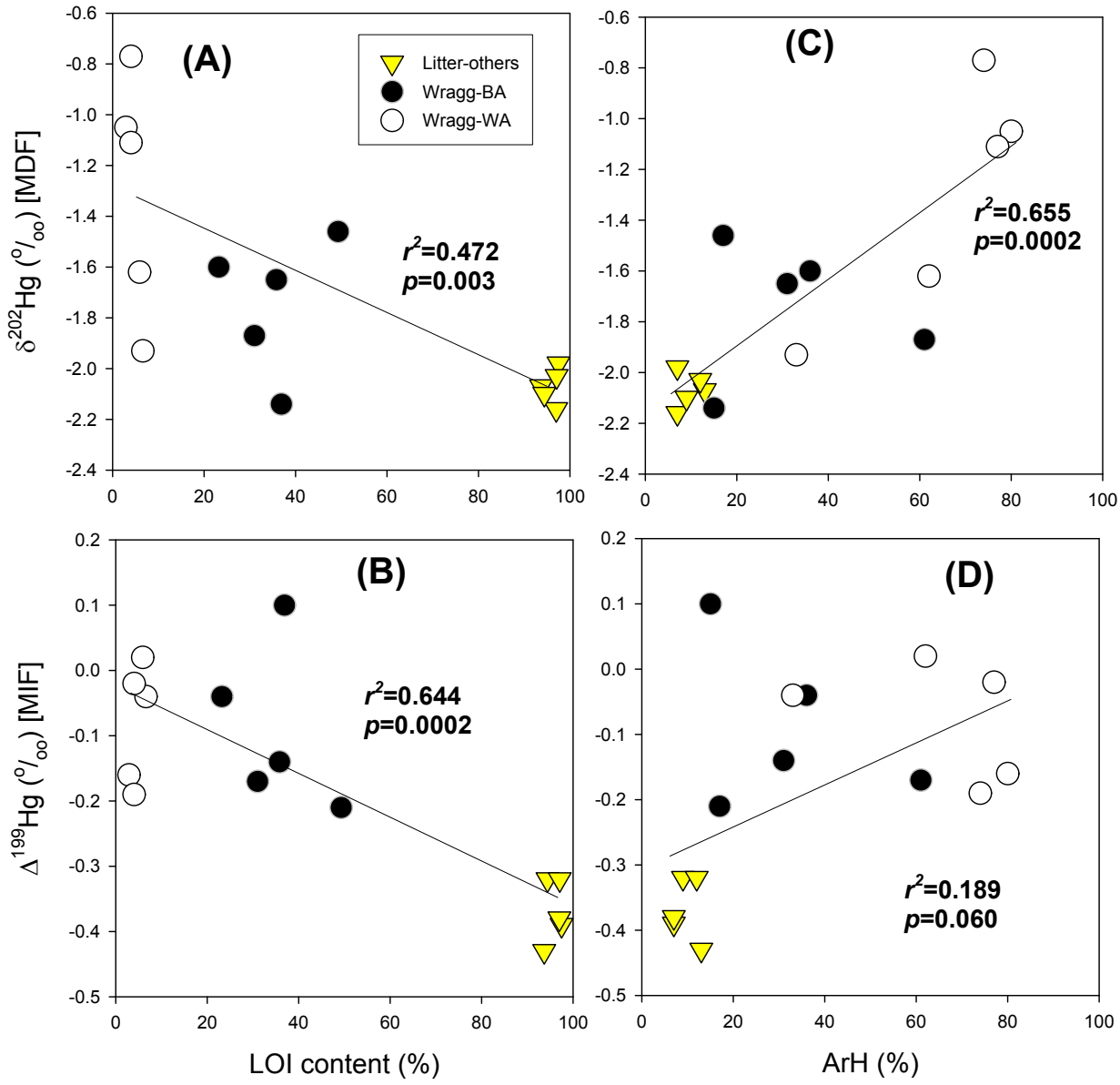

Fig. S3 Relationships between loss-on-ignition (LOI) and **(A)** δ^{202}Hg (mass-dependent fractionation [MDF]), and **(B)** Δ^{199}Hg (mass-independent fractionation [MIF]) of Hg isotopes among different unburned litter and ash samples. Relationships between percent of aromatic hydrocarbon (ArH) of pyrolysis products content and **(C)** δ^{202}Hg (mass-dependent fractionation [MDF]), and **(D)** Δ^{199}Hg (mass-independent fractionation [MIF]) of Hg isotopes among different unburned and ash samples. Published isotope data of foliage was not included as that particular study[15] did not provide information on LOI and ArH.

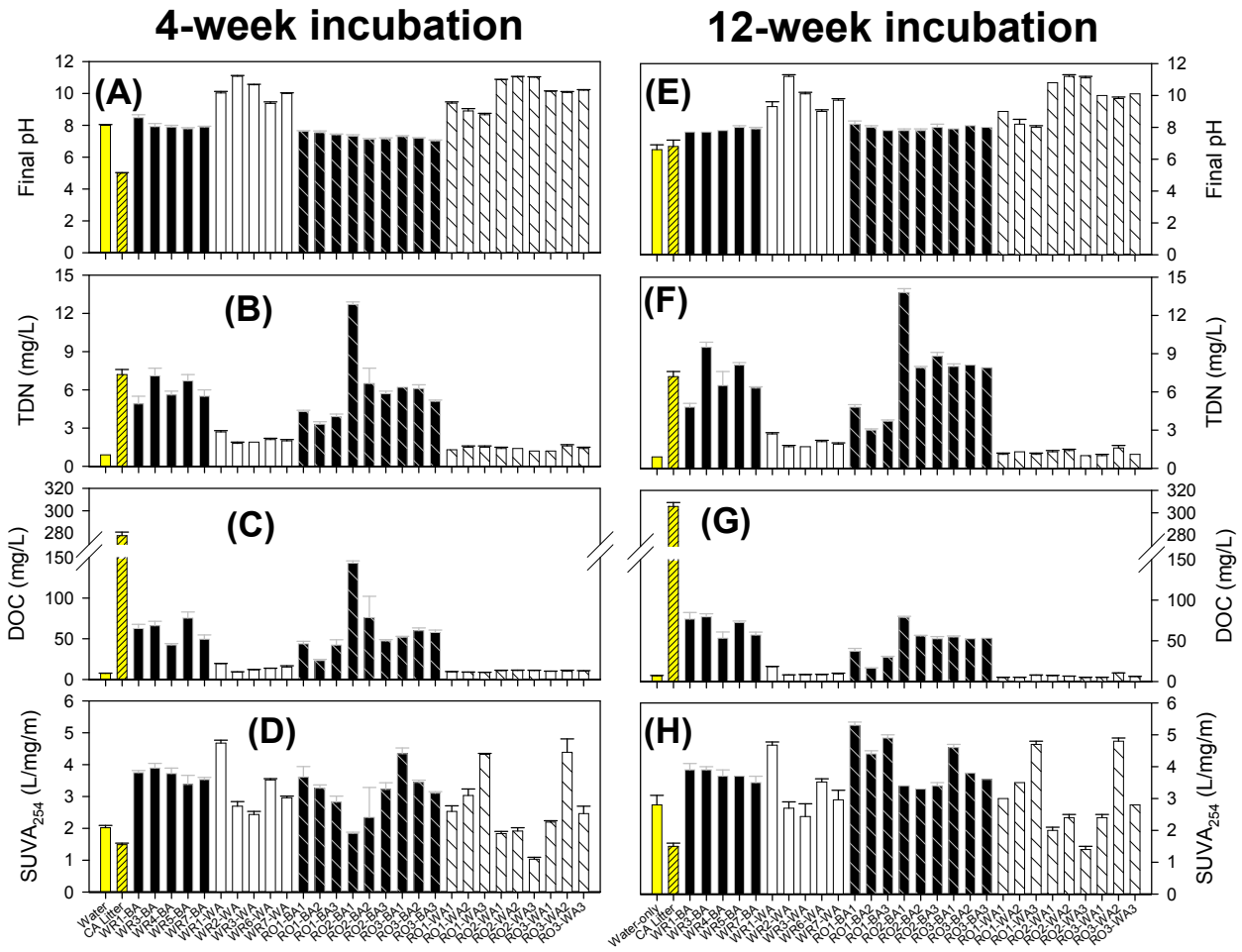

Fig. S4 Data from incubation experiment for 4-week and 12-week, data are mean±s.d. (*n*=3; except RO3-BA2 and RO3-BA3 where n=1). **(A, E)** final pH at 4- and 12-week; **(B, F)** total dissolved nitrogen (TDN) at 4- and 12-week; **(C, G)** dissolved organic carbon (DOC) at 4- and 12-week; and **(D, H)** proxy of DOC aromaticity ($SUVA_{254}$) of the aqueous phase at 4- and 12-week. Note: Yellow: water-only; Hatched yellow: unburned litter from a northern California forest (Angelo Reserve); Black: BA from Wragg; White: WA from Wragg; Hatched black: BA from Rocky; Hatched white: WA from Rocky.

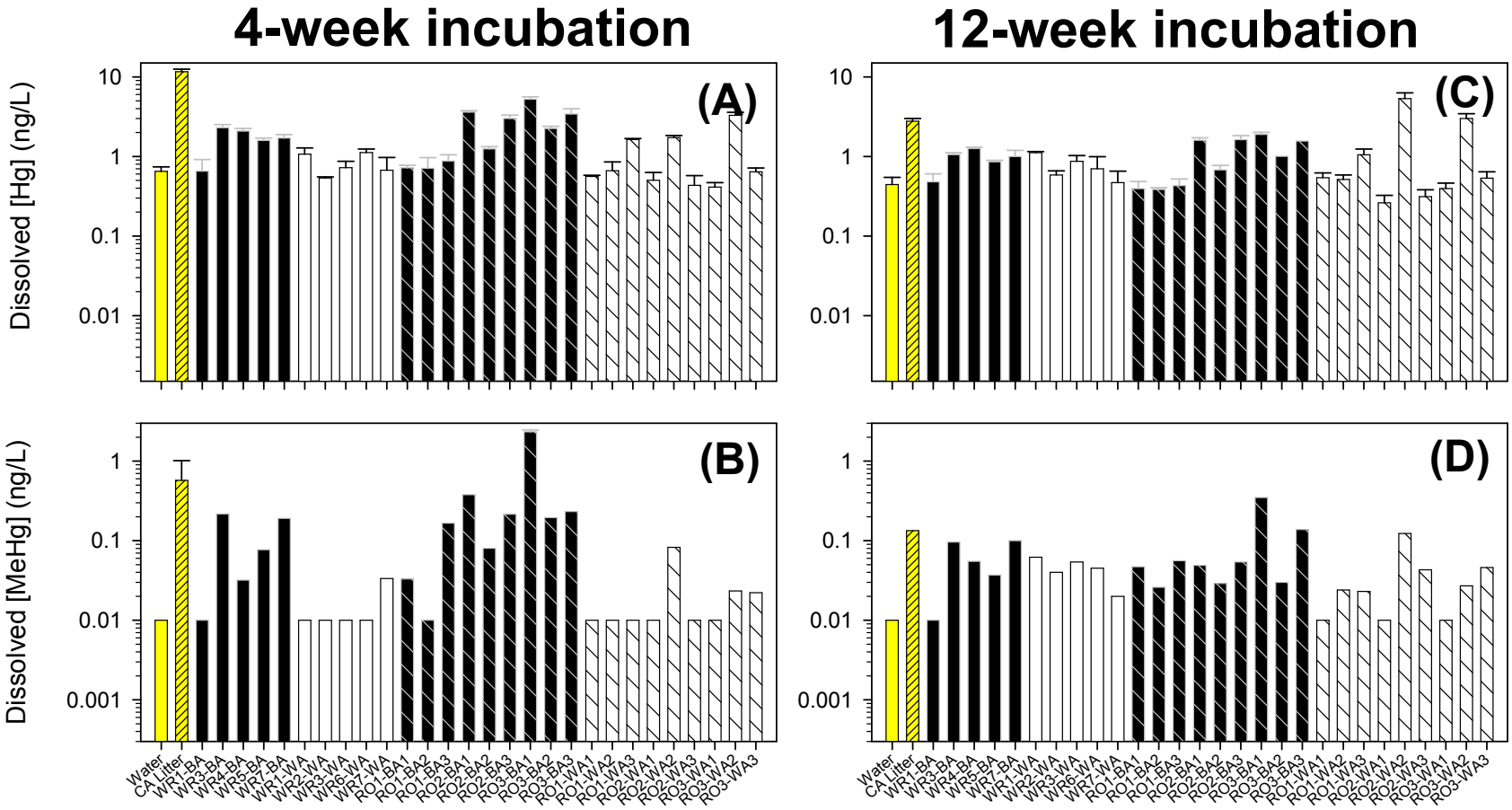

Fig. S5 Concentrations of dissolved (<1-μm) mercury concentrations ([Hg]; **A** and **C**) and dissolved methylmercury concentrations ([MeHg]; **B** and **D**) after 4- or 12-weeks of sealed incubation from water only (filtered stream water only, no solid materials added), unburned California litter (CA Litter), Wragg Fire black ash (WRX-BA), Wragg Fire white ash (WRX-WA), Rocky Fire black ash (RO#-BA), and Rocky Fire white ash (RO#-WA), where # is the site locations. Data are mean±s.d. (n=3 for Hg data while n=1 for most MeHg data).

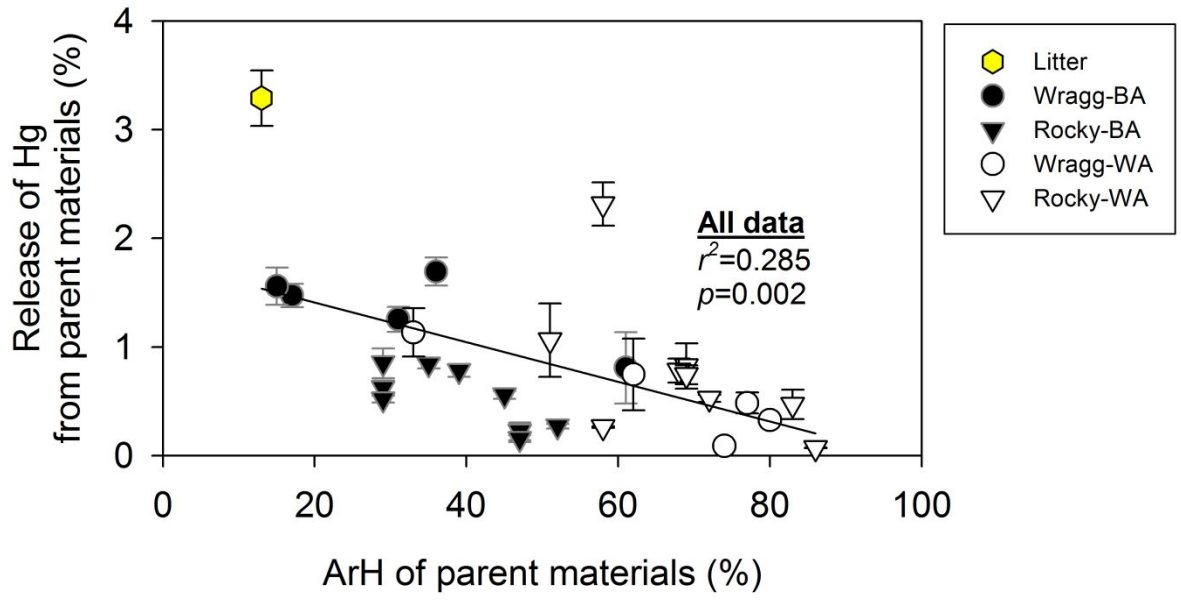

Fig. S6 Relationships among parameters after 4 weeks of sealed incubation experiment. Release of Hg from parent materials as a function of percent aromatic hydrocarbon (ArH) content of pyrolysis products.

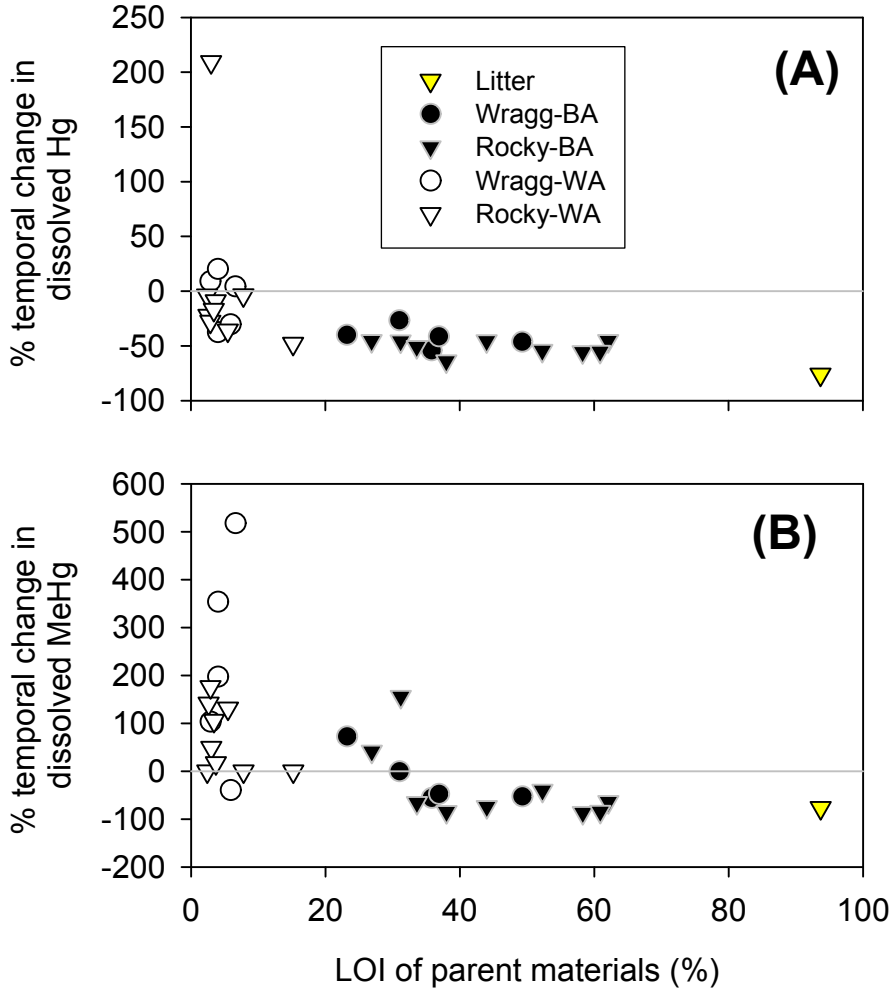

Fig. S7 Temporal percent changes of dissolved **(A)** mercury (Hg) and **(B)** methylmercury (MeHg) concentrations in incubation bottles from 4-weeks to 12-weeks among incubation materials of different loss-on-ignition (LOI).

SI References

1. Olund, S. D.; DeWild, J. F.; Olson, M. L.; Tate, M. T. Methods for the preparation and analysis of solids and suspended solids for total mercury. Chapter 8 of Book 5, Laboratory Analysis Section A, Water Analysis. 2004. U.S. Geological Survey, Reston, Virginia.
2. Song, J., Peng, P. A. Characterisation of black carbon materials by pyrolysis–gas chromatography–mass spectrometry. *J. Anal. Appl. Pyrolysis* **2010**, *87*, 129-137.
3. Chen, H.; Blosser, G. D.; Majidzadeh, H.; Liu, X.; Conner, W. H.; Chow, A. T. Integration of an automated identification-quantification pipeline and statistical techniques for pyrolysis GC/MS tracking of the molecular fingerprints of natural organic matter. *J. Anal. Appl. Pyrolysis* **2018**, *143*, 371-380.
4. Blum, J. D.; Bergquist, B. A. Reporting of variations in the natural isotopic composition of mercury. *Anal. Bioanal. Chem.* **2007**, *388*, 353-359.
5. Demers, J. D.; Blum, J. D.; Zak, D. R. Mercury isotopes in a forested ecosystem: Implications for air-surface exchange dynamics and the global mercury cycle. *Glob. Biogeochem. Cycles* **2013**, *27*, 222-238.
6. Tsui, M. T. K.; Blum, J. D.; Kwon, S. Y.; Finlay, J. C.; Balogh, S. J.; Nollet, Y. H. Photodegradation of methylmercury in stream ecosystems. *Limnol. Oceanogr.* **2013**, *58*, 13-22.
7. Tsui, M. T. K.; Blum, J. D.; Finlay, J. C.; Balogh, S. J.; Nollet, Y. H.; Palen, W. J.; Power, M. E. Variation in terrestrial and aquatic sources of methylmercury in stream predators as revealed by stable mercury isotopes. *Environ. Sci. Technol.* **2014**, *48*, 10128-10135.
8. Woerndle, G. E.; Tsui, M. T. K.; Sebestyen, S. D.; Blum, J. D.; Nie, X.; Kolka, R. K. New insights on ecosystem mercury cycling revealed by Hg isotopic measurements in water flowing from a headwater peatland catchment. *Environ. Sci. Technol.* **2018**, *52*, 1854-1861.
9. Balogh, S. J.; Huang, Y.; Offerman, H. J.; Meyer, M. L.; Johnson, D. K. 2002. Episodes of elevated methylmercury concentrations in prairie streams. *Environ. Sci. Technol.* **2002**, *36*, 1665-1670.
10. Tsui, M. T. K.; Finlay, J. C.; Nater, E. A. Effects of stream water chemistry and tree species on release and methylation of mercury during litter decomposition. *Environ. Sci. Technol.* **2008**, *42*, 8692-8697.
11. Blum, P. W.; Hershey, A. E.; Tsui, M. T. K.; Hammerschmidt, C. R.; Agather, A. M. Methylmercury and methane production potentials in North Carolina Piedmont stream sediments. *Biogeochemistry* **2018**, *137*, 181-195.
12. Parker, J. L.; Bloom, N. S. Preservation and storage techniques for low-level aqueous mercury speciation. *Sci. Total Environ.* **2005**, *337*, 253-263.
13. Mitchell, C. P. J.; Branfireun, B. A.; Kolka, R. K. Spatial characteristics of net methylmercury production hot spots in peatlands. *Environ. Sci. Technol.* **2008**, *42*, 1010-1016.
14. Weishaar, J. L.; Aiken, G. R.; Bergamaschi, B. A.; Fram, M. S.; Fujii, R.; Mopper, K. Evaluation of specific ultraviolet absorbance as an indicator of the chemical composition and reactivity of dissolved organic carbon. *Environ. Sci. Technol.* **2003**, *37*, 4702-4708.
15. Zheng, W.; Obrist, D.; Weis, D.; Bergquist, B. A. Mercury isotope compositions across North American forests. *Glob. Biogeochem. Cycles* **2016**, *30*, 1475-1492.